Available online at www.sciencedirect.com
ScienceDirect
Palaeogeography, Palaeoclimatology, Palaeoecology 239 (2006) 426–455
PALAEO
www.elsevier.com/locate/palaeo

Chronostratigraphy of Late Neogene sediments in the southern North Sea Basin and paleoenvironmental interpretations

Gesa Kuhlmann [a,b], Cor Langereis [a,*], Dirk Munsterman [b], Robert Jan van Leeuwen [b], Roel Verreussel [b], Johan Meulenkamp [a], Theo Wong [a,b]

[a] *Department of Earth Sciences, Utrecht University, Budapestlaan 4, 3584 CD Utrecht, The Netherlands*
[b] *TNO-NITG, National Geological Survey of the Netherlands, Princetonlaan 6, 3584 CB Utrecht, The Netherlands*

Received 3 April 2005; received in revised form 9 January 2006; accepted 16 February 2006

Abstract

A chronostratigraphic framework has been established for Upper Neogene sediments from the northern Netherlands offshore sector, southern North Sea. Data of dinoflagellate cysts, pollen and foraminifers from eight boreholes are integrated and the resulting biostratigraphic events are connected to an additionally retrieved paleomagnetic record. The sedimentary succession comprises at the base Late to Middle Miocene sediments and spans the Piacenzian to Gelasian stages, from 3.6 to 1.8 Ma, including the paleomagnetic Gauss–Matuyama boundary and the Olduvai subchron. Sedimentation rates vary between 30 cm/kyr in the lower part of the succession and reach up to 84 cm/kyr in the upper part. These rates are high enough to record short paleomagnetic events and for the first time the presence of the so-called X-event has been recorded and dated at around 2.44 Ma in a sedimentary setting. The name ‘North Sea event’ is proposed here. The paleoclimatic and paleoenvironmental information pictures the onset of Northern Hemisphere Glaciation and the subsequent intensification of glacial conditions with its impact on the North Sea sea region. The paleoenvironmental changes are characterised by a stepwise development and five successive intervals are distinguished. During the first interval, a warm climate and an open marine setting prevailed. The second interval is characterised by dominantly cold climatic conditions with occasional warmer periods. During the third interval, the environment became restricted marine and a stable freshwater layering occurred, which facilitated the development of sea-ice in the shallow sea. Within the fourth interval, extreme cold (arctic) conditions were predominant, and shallowing continued. The fifth interval shows fluvial to deltaic, paralic conditions. From then on, facies differences from the nearby delta system overruled the basin-wide signals at the studied location.

Keywords: North Sea; Neogene; Paleoenvironment; paleomagnetism; biostratigraphy; chronostratigraphy; X-event

1. Introduction

During Cenozoic times, the central North Sea Basin was filled with more than 3 km of siliciclastic sediments (Fig. 1a; Ziegler, 1990). Half of this sedimentary succession was deposited during the ~15 my Neogene period. Although the search for hydrocarbons has generated a wealth of information on North Sea geology (Parker, 1993; Fleet and Boldey, 1999; Evans et al., 2003), relative little attention has been paid to the Upper Cenozoic deposits. This is due to their position far above

* Corresponding author.
E-mail address: langer@geo.uu.nl (C. Langereis).

0031-0182/$ - see front matter © 2006 Elsevier B.V. All rights reserved.
doi:10.1016/j.palaeo.2006.02.004

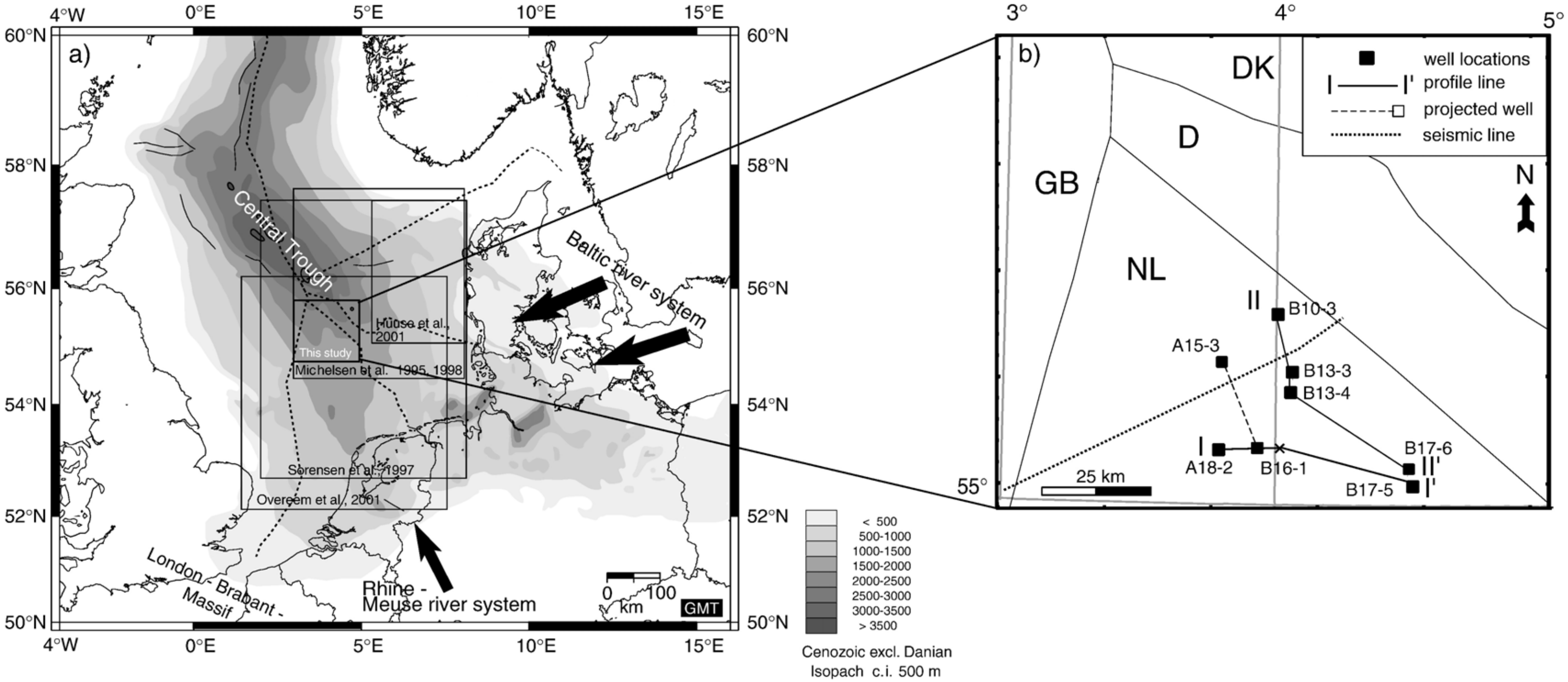

Fig. 1. a) Map showing the study area and relevant areas mentioned in the text within the southern North Sea. The Late Cenozoic basin infill is superimposed on the present day land–sea contours (isopach map after Huuse et al., 2001). b) Details of the study area including the national sector boundaries. The locations for the eighth wells used for biostratigraphic analyses are shown with closed squares. Paleomagnetic data have been obtained from well A15-3 (this study) and in well B16-1 (cross) (Barthés et al., 1999). The locations of the two well log correlation profiles presented in Fig. 3 and the seismic profile presented in Fig. 10 are indicated. Note that the open square is a projection of the well onto the profile line. 1 = This study, 2 = Michelsen et al. (1995) and (1998), 3 = Sørensen et al. (1997), 4 = Overeem et al. (2001), 5 = Huuse et al. (2001). The two main river systems (Baltic and Rhine–Meuse) contributing to sedimentation during the Pliocene are indicated by arrows.

the main hydrocarbon findings on the one hand, and their location too deep below the seabed for research by others than oil companies on the other hand. However, due to the recent discovery of shallow gas in Neogene sediments in the Netherlands offshore sector, exploration activity has been initiated, leading to a large number of high quality borehole samples, used for this study.

Numerous biostratigraphical studies of Cenozoic sediments from the North Sea Basin have been published (Doppert, 1980; Gradstein and Berggren, 1981; King, 1983; Cameron et al., 1984; Vinken, 1988; King, 1989; Gibbard et al., 1991; Gradstein et al., 1992, 1994; Laursen, 1995; Konradi, 1996; and Eidvin et al., 1999). From studies dealing with Cenozoic sequence stratigraphy of the North Sea (Cameron et al., 1987, 1993; Michelsen et al., 1995; Jordt et al., 1995), the architecture of the sedimentary structures has become better known. Michelsen et al. (1995) established a first sequence stratigraphic framework for the entire Cenozoic succession based on the integration of logstratigraphy, seismic stratigraphy and biostratigraphy. This framework was further improved by detailed studies concerning the Late Cenozoic of the central and southern North Sea Basin (Sørensen and Michelsen, 1995; Sørensen et al., 1997; Michelsen et al., 1998; Overeem et al., 2001).

A comprehensive chronostratigraphy of the Neogene is difficult to establish within the North Sea Basin because of the progradational character of the Miocene and Pliocene sediments. Towards the eastern part of the North Sea (i.e. Danish and German sectors), Miocene sediments are more complete, while Pliocene sediments are deposited more towards the west and north (i.e. Dutch and Norwegian sectors). Moreover, age assessments of the sediments in the offshore region are mainly based on biostratigraphic data from low quality samples, such as ditch cuttings from exploration wells. Therefore, the data integrated so far into standard zonations lacks the resolution required for detailed studies of the Pliocene. Control on absolute ages is even scarcer. Only one continuous paleomagnetic record has been retrieved in an

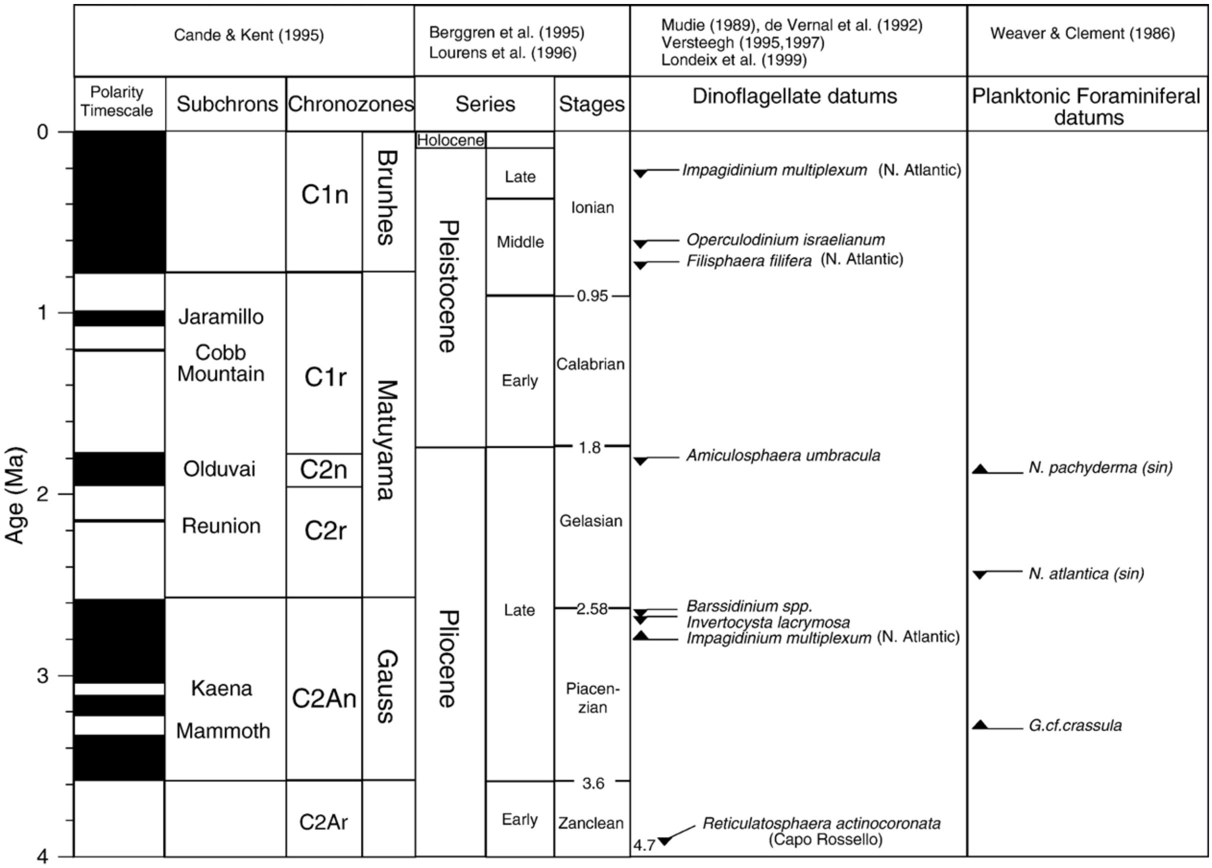

Fig. 2. Standard chronostratigraphy related to the global polarity time scale (GPTS) and calibrated dinoflagellate and planktonic foraminiferal datums. The chronostratigraphy is based on Cande and Kent (1995), Berggren et al. (1995) and Lourens et al. (1996). The biostratigraphic datums are taken from Mudie (1989), De Vernal et al. (2001), Versteegh (1995), Londeix et al. (1999) and Weaver and Clement (1986).

exploration well in the southern North Sea (Barthés et al., 1999). Because a solid chronology is essential for the understanding of the basin development as well as of the geological processes controlling the stratigraphic sequences, a detailed study has been carried out using dinoflagellates, foraminifers and pollen. The resulting biostratigraphic framework is linked to a paleomagnetic record established in this study. Additionally, the investigated fossil groups were used as proxies for paleoenvironmental interpretations.

Harland (1992) and Cameron et al. (1984) have demonstrated that dinoflagellate cysts show potentially useful stratigraphical datums in the North Sea Basin. Through the studies from the North Atlantic (Harland, 1979; Mudie, 1989; De Vernal et al., 1992; Versteegh, 1995; Matthiessen and Brenner, 1996; Poulsen et al., 1996; Smelror, 1999), the dinocyst record of the southern North Sea Basin can be connected to the global standard record (Fig. 2). All studies indicate that many dinocyst species became extinct in the course of the Plio-Pleistocene, while only few species have their first appearance in that time interval. Because motile dinoflagellates are most abundant in nutrient-enriched waters, like marginal seas and oceanic fronts, they make up an important part of the plankton within the North Sea region. Therefore, changing properties of watermasses are generally well reflected in the fossil dinocyst record (Edwards and Andrle, 1992; Rochon et al., 1999; De Vernal et al., 2001).

Pollen and spores are allochthonous components of the marine sediments. In our interpretation we assume that the majority of the pollen and spores is primarily transported by rivers rather than by wind. Despite the fact that stratigraphic utility of pollen assemblages is limited in offshore regions, useful climatic information can be derived from the pollen signal.

Foraminiferal zonations for the North Sea region have been compiled for the Miocene to Pliocene by Doppert (1980), King (1983, 1989) and Eidvin et al. (1999). Although planktic species are very scarce in the Upper Cenozoic of the North Sea, some datums are linked to magnetostratigraphically dated sections in the North Atlantic (Weaver and Clement, 1986; Fig. 2). At the same time, environmental changes are well recorded by the benthic foraminiferal assemblages since they respond to changes in the sediment as well as to changes in the water column.

For our detailed study of the North Sea Neogene, we investigated sedimentary sections from eight boreholes of the northernmost Dutch offshore sector using dinoflagellates, foraminifers and pollen. A paleomagnetic record was retrieved in one borehole using the Geological High-Resolution Magnetic tool (GHMT); additionally, paleomagnetic measurements were done on discrete samples. The samples for this study were provided by Wintershall Noordzee B.V. and the Nederlandse Aardoliemaatschappij (NAM). We integrated the new stratigraphic data of the different disciplines to define a chronostratigraphic framework for the Middle Miocene to Pliocene sediments. Furthermore, the paleoclimatic and paleoenvironmental information provided by the biota is interpreted in terms of climate change and changes in the oceanographic setting.

2. Geological setting

During Late Cenozoic times, the North Sea Basin, together with the East-German Polish Basin, was part of the North West European Basin (Vinken, 1988; Ziegler, 1990; Evans et al., 2003) covering the present day offshore and onshore parts of the Netherlands, Germany and Denmark. The basin was confined by landmasses, except towards the north-west, where it opened into the Atlantic (Bijlsma, 1981; Glennie, 1990; Ziegler, 1990) (Fig. 1a). Towards the south, the London–Brabant-Massif separated the North Sea Basin from the Atlantic, although at some times during the Pliocene a connection through the English Channel may have existed (Funnel, 1996).

The study area is situated in the southern part of the present day North Sea and comprises the northern part of the Netherlands offshore territory (Fig. 1b). Late Cenozoic sedimentation in the North Sea Basin was dominated by a large clastic depositional system that progressively prograded into the basin. This system probably existed in outline since Late Oligocene times (Burger, 2002; Huuse, 2002). Initially, the prograding system developed from the north-east, and then it rotated clockwise towards a sediment transport direction from the east and south-east (Sørensen et al., 1997; Michelsen et al., 1998; Clausen et al., 1999; Huuse et al., 2001). At these times, the sediments were mainly delivered by rivers draining the Fennoscandian Shield and the Baltic Platform (Bijlsma, 1981). This Baltic river system (Zagwijn, 1989; Gibbard et al., 1991) had an averaged drainage area of 1.100.000 km^2 (Overeem et al., 2001) and was active until the Late Pliocene, when it merged with the Rhine–Meuse river system, draining from the south-east (Fig. 1a).

Progradation of the sediments resulted in several major sequences within the Cenozoic in the North Sea Basin (Michelsen et al., 1998). One major sequence boundary is observed during the Middle Miocene, the so-called Mid-Miocene Unconformity (MMU) (Huuse and Clausen, 2001). The MMU is a transgressional surface that is characterised by sediment starvation and/or condensation during the late Middle Miocene (Huuse et al., 2001). It appears on seismic profiles as an onlap surface towards the north-east, as a prominent downlap surface within the southern North Sea region and as a conformable surface in the Central Trough (Cameron et al., 1993; Huuse and Clausen, 2001). Within the Danish sector, the age of the MMU is estimated at 12.4 Ma by Michelsen et al. (1998) and between 14 to 15 Ma by Huuse and Clausen (2001). In the southern Norwegian sector, the top of the unconformity is dated at 11.2 Ma (Eidvin et al., 1999) and in the German sector at 10.7 Ma (Streif, 1996). These data imply that the age of the onset of sedimentation on top of the MMU decreases with the progradational direction of the sediments. There is still ongoing debate on the origin of the MMU: it might have resulted from a relative sea-level rise, either eustatic in combination with tectonic subsidence (Gramann and Kockel, 1988; Kooi et al., 1991; Cameron et al., 1993), or from a sudden increase in sediment input into an already deep marine basin caused by climatic changes (Huuse and Clausen, 2001).

After the Middle Miocene sea level highstand, the central and southern parts of the North Sea were probably a relatively deep part of the epicontinental sea with estimated maximum water depths between 130 and 400 m, as deduced from seismic clinoforms (Gramann and Kockel, 1988; Cameron et al., 1993; Overeem et al., 2001; Huuse, 2002). During the Middle Miocene, the studied area received relatively little sediment, as it was distal to the main locus of sedimentation. As progradation continued, sedimentation rates in the central part of the North Sea steadily increased and in Pliocene times the core of the depositional system reached the area of the present study (Sørensen et al., 1997; Overeem et al., 2001). From the Late Pliocene onward, the sea rapidly shallowed and depth differences were levelled off.

By Middle Pleistocene times, a large delta plain had come into existence covering an area of some 150.000 km^2 towards the south and east, and only in the central North Sea marine sedimentation continued (Cameron et al., 1993). Middle to Late Pleistocene sedimentation was dominated by climatic changes, ice sheets completely altered the drainage pattern and the river systems ceased to exist around 450.000 years ago (Zagwijn, 1989). During glacial maxima, ice sheets reached the area more than once and glacially controlled sea level changes had profound effects on sedimentation in the shallow basin. The sedimentation became increasingly discontinuous with glacial channels as common erosional features (Cameron et al., 1993; Huuse et al., 2001; Huuse, 2002).

3. Materials and methods

For biostratigraphical analyses, samples were taken from eight different exploration wells (Fig. 1b, Table 1). Most of the samples were from sidewall cores and cores; ditch cuttings were taken only when no other material was available. The analyses included the quantitative studies of dinoflagellate, pollen and foraminiferal assemblages. Lithology was determined by visual core and sample descriptions.

For dinoflagellate cyst analyses, the samples were treated with 30% hydrochloric acid (HCl) to dissolve the carbonates. To remove the silicates, the residue was treated with hydrofluoric acid (HF). Afterwards, the fluoride gel was removed with 30% HCl and the organic residue was concentrated using an 18 μm sieve. Finally, heavy liquid separation ($ZnCl_2$, specific gravity: 2.1 g/cm^3) was applied. The organic residue was mounted on slides and up to 100 specimens were determined and counted.

The samples for pollen analysis were decalcified with 10% HCl. Excess organic material was removed with

Table 1
Well names with number and quality of investigated samples (HQ = high quality as core samples and sidewall core samples, LQ = low quality as ditch cuttings)

Well	Company	Pollen	Dinocysts		Forams		Paleomagnetics
		HQ	HQ	LQ	HQ	LQ	
A15-3	Wintershall		15	40			GHMT, 91 samples
A18-2	NAM	56					
B10-3	NAM	46	19		46	14	
B13-3	NAM	68	24		29	10	
B13-4	NAM		21				
B16-1	NAM	29	29				Barthés et al. (1999)
B17-5	NAM	49			40	3	
B17-6	Wintershall		7	28			

10% potassium hydroxide (KOH) and afterwards the samples were acetolyzed to colour the sporomorphs. A bromoform solution (specific gravity 2.1 g/cm^3) was used for heavy liquid separation to remove the silicates and heavy minerals. After sieving, the fraction between 7 and 125 μm remained. This organic residue was mounted on slides and if possible, a total amount of 200 pollen grains was counted at each level.

For foraminiferal analyses the sediments were oven-dried, weighed and washed over a set of sieves with mesh size of 840 and 125 μm. The residues were dried again and large residues were split until an aliquot containing a minimum of 100 foraminifers was obtained. Analysis of the foraminiferal assemblages was based on the > 125 μm fraction. All foraminifers and Bolboforma were subsequently picked under the binocular microscope. All biostratigraphic data are reported in Appendix A (dinocyst data), Appendix B (pollen data) and Appendix C (foraminifer data).

Paleomagnetic analyses involved the use of the downhole Geological High-Resolution Magnetic Tool (GHMT) and paleomagnetic measurements on discrete core samples of one borehole. The processing of the GHMT data and interpretation was done by Schlumberger-Geoquest (France); the processing procedure used is described in more detail by Pozzi et al. (1993) and Etchecopar et al. (1994). The GHMT was run over an interval from 430 to 1246 m, where the signal from 441 m depth downwards was used for the interpretation because the casing in the upper part of the borehole prevented valid measurements. Sediment samples from both cores and sidewall cores (Fig. 7) were taken separately and measured in orientated standard plexiglas cylinders. The susceptibility of the discrete samples was measured on a Kappabridge (KLY-3). These results were used to adjust the cored depth to the logged depth by matching them to the susceptibility log of the GHMT. The natural remanent magnetisation (NRM) was measured on a DC SQUID cryogenic magnetometer (2G-Enterprises). All samples were thermally demagnetised with temperature steps of 20–30 °C up to a maximum of 560 °C. Additionally, the sidewall cores were progressively demagnetised along three axes in alternating fields (AF) up to 70 mT. At fields higher than 40 mT, the samples began to acquire a gyroremanent magnetisation, masking the NRM signal. Using the approach by Dankers and Zijderveld (1981), the samples were measured after each axis was separately demagnetised. For interpretation, Zijderveld plots (Zijderveld, 1967; Langereis et al., 1989) were used. Only inclination was taken for interpreting the magnetic polarities because the azimuth of the cores is not known. Finally, the results of the discrete samples were taken to adjust and calibrate the processing of the results obtained by the GHMT-tool.

For logstratigraphical interpretations and correlation between the eight investigated boreholes, gamma-ray records were used (Fig. 3). Since the gamma-ray response records sediment attributes (i.e. the radioactivity of uranium, thorium, and potassium), correlation of the signal may represent facies-dependent, diachronous features. Nevertheless, correlation of the biostratigraphic data (Kuhlmann, 2004) showed congruency between log correlation and the biostratigraphical datums. Therefore, the correlative logstratigraphical units are assumed to represent time equivalent horizons. Subsequently, the similar gamma-ray log pattern in seven out of eight wells was used to construct a composite record. Through the integrated bio- and logstratigraphic framework, the variable sample spacing (Fig. 3) could be compensated for and two boreholes with deviating gamma-ray log pattern (B17-5, B17-6) could be placed within the logstratigraphic context.

4. Results

4.1. Logstratigraphy

In former studies (cf. Sørensen et al., 1997), the Mid-Miocene unconformity (MMU) has been identified as a prominent high in the gamma-ray log. In four of our studied wells, this marker horizon was reached in the signal (Fig. 3). Contrary to Sørensen et al. (1997), who applied the sequence stratigraphic concepts of Vail (1987) and Van Wagoner et al. (1990), we defined logstratigraphical units in a more descriptive way. Unit boundaries were placed at both, trend reversals and distinct gamma-ray log breaks. Despite the fact that the gamma-ray peak represents the MMU (Kristofferson and Bang, 1982), we placed the logmarker for consistency reasons with Sørensen et al. (1997) directly beneath this peak. Eighteen logstratigraphical units, shortly named logunits, have been discriminated (Fig. 3). They comprise the interval from the MMU to a depth above which log correlation becomes unreliable as the presence of casing disturbed the log signal. In spite of the different approach, most of the units described in this study can be unambiguously correlated with the sequence stratigraphic units of Sørensen et al. (1997) (Fig. 9) and represent chronostratigraphic units.

The lowest part of the investigated succession, i.e. logunit 1, comprises the highly condensed interval of the four composite sequences I to IV described by Sørensen et al. (1997). In most of the wells, the following part of the succession, consisting of logunits 2 and 3, is

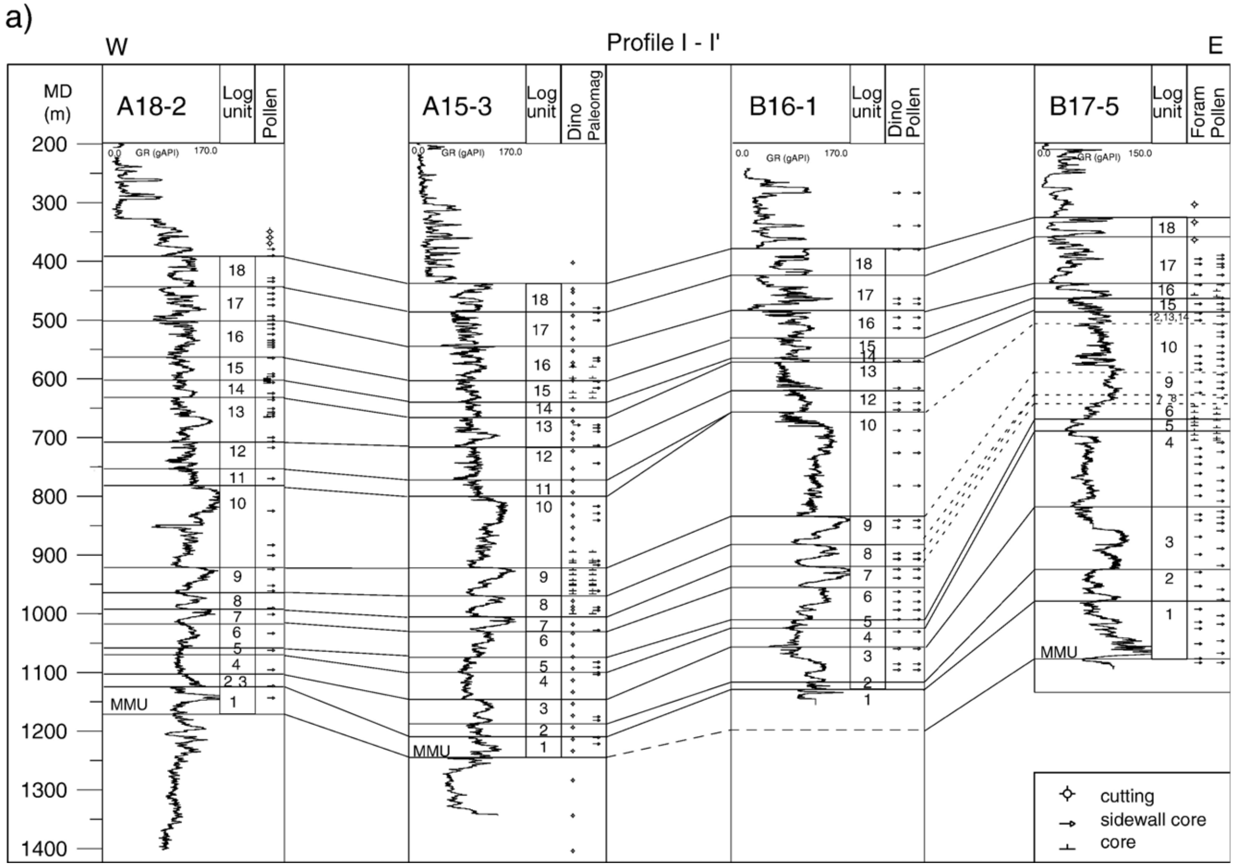

Fig. 3. a) West–East profile (I–I′) and b) north–south profile (II–II′), showing the gamma-ray log response and the correlation of the wells used for this study with the sample density per well.

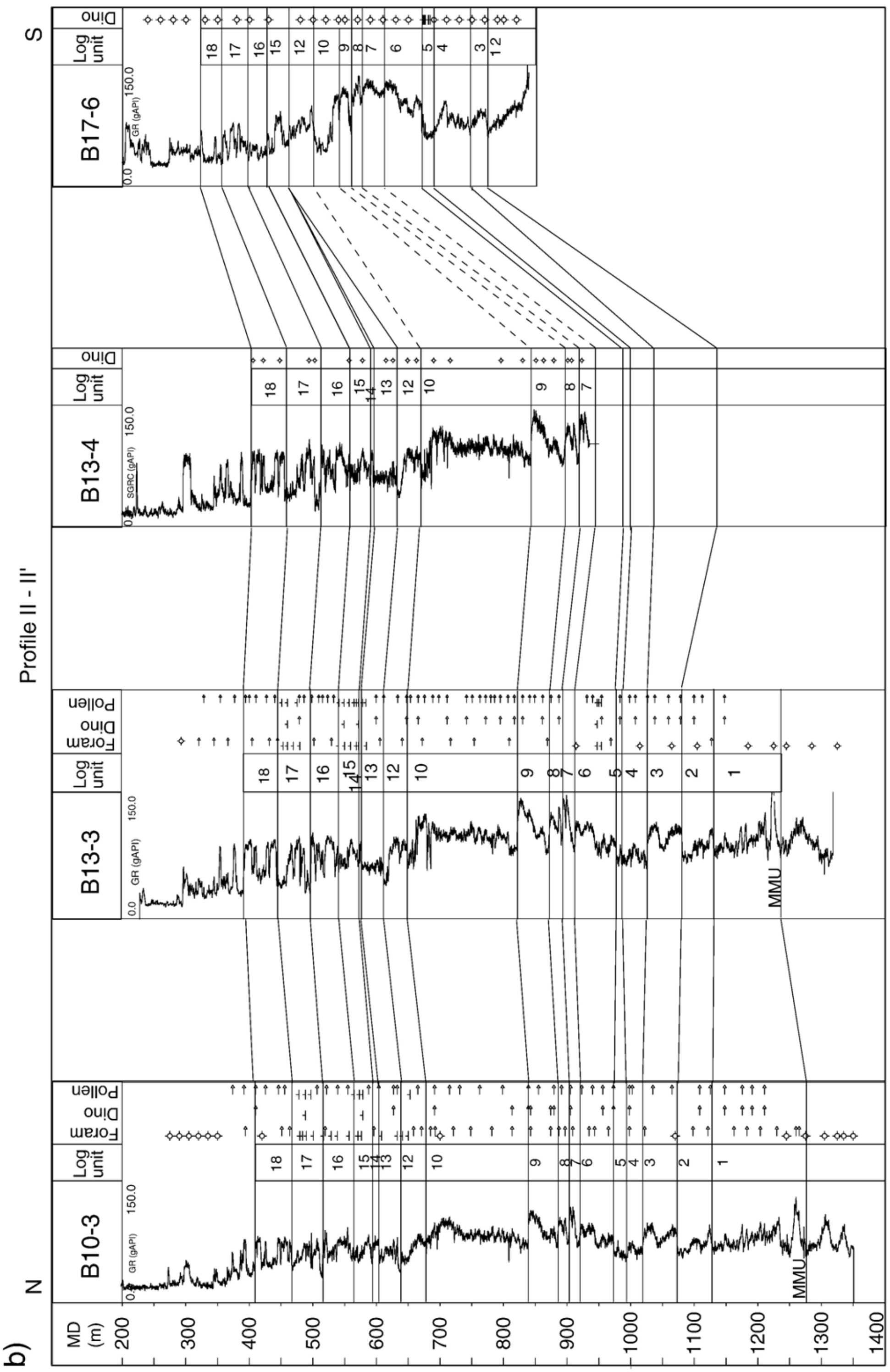

Fig. 3 (continued).

condensed as well. Stratigraphic resolution is therefore lower than in the interval lying above. For this reason, our study focuses on logunits 4 to 17. The gamma-ray log response is very similar in six of the eight wells; only the two most easterly wells, B17-5 and B17-6, show a deviating log response (Fig. 3), probably caused by their location above a salt dome and their more proximal setting to the shoreline. In these two wells, logunits 4 and 5 are up to three times as thick as in the other wells, which might be because of the position more in the east and thus represent parts of prograding units that occur more to the east. The signal of the upper part of these wells (logunits 7 to 18), however, is more difficult to correlate (Kuhlmann, 2004) as it is approximately half as thick as in the westernmost wells, representing condensed sediments or hiatuses due to erosion and bypass of the sediments.

From the gamma-ray log and lithological descriptions it is inferred that the lower and middle parts of the succession (logunits 1 to 12) mainly consist of silt, silty clays and clayey silts. From logunit 13 upward, very thin fine sandy layers start to intercalate with the silty to clayey sediments. Variable gamma-ray values are present up to logunit 12 (Fig. 3) the decreasing trend of the gamma-ray from logunit 13 onward represents the coarsening upwards as seen in the sediments. In the lower part of the succession (logunits 1 to 4), the gamma-ray logs show coarsening upward sequences within the logunits, while from logunit 5 the trend is reversed and shows fining upward trends within the logunits culminating in a gamma-ray peak of logunit 10. From this point, the fining upward trend abruptly ends and erosional surfaces can be observed within the upper part of the succession, i.e. at the base of logunit 11 and 13 (Fig. 3).

4.2. Dinoflagellates

Based on dinoflagellate countings in six boreholes, the thirteen most consistent events are listed as D1 to D13 in the composite record of Fig. 4. Together with other events they are described below. Most events are quantitative and can directly be related to local or regional changes in the paleoenvironment and reflect changes even on a global scale.

The assemblages pre-dating the MMU include *Apteodinium spiridoides*, *Palaeocystodinium ventricosum* and *Unipontidinium aquaeductum*. Logunits 1 and 2, as part of the condensed interval, yield mainly undiagnostic *Spiniferites*-dominated assemblages up to the last occurrence datum (LOD) of *Melitasphaeridium choanophorum* (D1) at the base of logunit 3. *Amiculosphaera umbracula* and *Operculodinium eirikianum* are quite common. The LODs of *Reticulosphaera actinocoronata* and *Operculodinium piaseckii* are recorded in the lower part of this interval.

Between logunits 3 and 5 (D1 and D2) reworked palynomorphs or fresh-water algae are rare to absent. The diverse dinocyst assemblage in this interval is dominated by *Spiniferites*, although a distinct decrease of this species is observed towards the top (D2). The distribution pattern of *Bitectatodinium tepikiense* however, displays an increase towards the top. The occurrence of *Nematosphaeropsis lemniscata* is restricted to the lower part of the interval. A conspicuous feature is the (near) absence of *O. eirikianum*, while *Operculodinium centrocarpum* is commonly present. *Operculodinium israelianum*, on the other hand, occurs in moderate numbers. *Lingulodinium machaerophorum* is often abundant, but its distribution pattern is irregular. *Achomosphaera andalousiensis* reaches its highest values (still below 10%) in this interval, while *Filisphaera* and *Habibacysta* are very rare. *Barssidinium* spp. (D2) has its LOD at the top of this interval. At the same level, various other taxa have their last consistent occurrence, e.g. *Batiacasphaera minuta*, *Heteraulacacysta* spp., *A. andalousiensis* ssp. *suttonensis* and *Barssidinium* spp. The last consistent occurrence of the extant taxon *Tectatodinium pellitum* is recorded approximately in the middle of this interval.

In the lower part of logunit 6, the thin interval between dinoflagellate events D2 and D3, the assemblages are characterised by an acme occurrence of *L. machaerophorum* as well as high abundance of *O. centrocarpum*. *Impagidinium multiplexum* has its FOD at the base of this interval (D2).

In most of the interval from the upper part of logunit 6 to the lower part of logunit 10 (D3 to D7) the overall diversity remains high, but the dinocyst assemblages are no longer dominated by *Spiniferites*. The assemblages are rich and diverse with common *Spiniferites*, *L. machaerophorum*, *O. centrocarpum*, *O. israelianum*, *O. eirikianum* and *B. tepikiense*. The *Filisphaera*/*Habibacysta* group (D3 to D4) is predominantly present while *O. centrocarpum* and *L. machaerophorum* are quite common. In well A15-3, *O. centrocarpum* and the *Filisphaera*/*Habibacysta* group are equally abundant present. *O. israelianum* and *I. multiplexum* are generally rare (below 10%). The overall levels of reworking are low except of two distinct peak occurrences of reworking in logunit 6 and 9. *A. umbracula*, *O. eirikianum* and *Brigantedinium* spp.('round browns') are consistently present, except in well B17-6. An acme of *I. multiplexum* (D5) is recorded in logunit 9, the highest abundance (>20%) of *I. multiplexum* is seen in the wells B17-6,

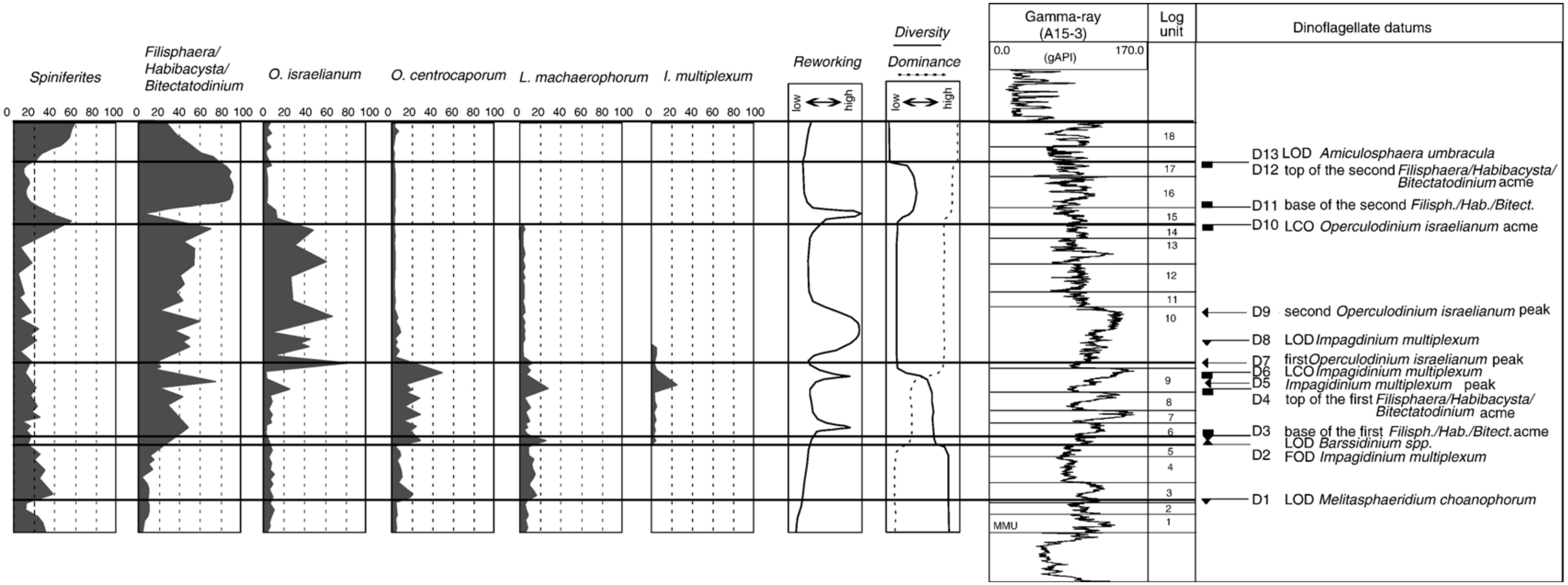

Fig. 4. Schematic diagram of the dinoflagellate results for the composite sections showing the 13 most important events and their stratigraphic position related to the gamma-ray log. Abbreviations: LOD = Last Occurrence Datum, LCO = Last Common Occurrence, FOD = First Occurrence Datum, FCO = First Common Occurrence.

B10-3 and B13-3; in the other wells *I. multiplexum* does not exceed (10%). Above the *I. multiplexum* acme, from the upper part of logunit 9, impoverished, low diversity, dinocyst assemblages occur. The LOD of *O. eirikianum* and the LOD of the very rare *Lejeunecysta catoma* coincide with this acme. Apart from *I. multiplexum*, the assemblages consist of a reworked component, 'round browns', and *O. centrocarpum*. At the top of logunit 9, *I. multiplexum* is no longer consistently present (D6) and the assemblages become completely dominated by *O. centrocarpum*. The *Filisphaera*/*Habibacysta* group is nearly absent.

At the base of the interval from logunit 10 to 14 (D7 to D10) a short but pronounced (>90%) acme of *O. israelianum* occurs (D7). This event represents an important break in the dinocyst record. The dinocyst assemblages at and above the D7 marker are characterised by high dominance and low diversity. The dinocyst assemblages mainly consist of *O. israelianum* and the *Filisphaera*/*Habibacysta* group, while *Spiniferites* may be common and *O. centrocarpum* and round browns may be present in low numbers. In the middle of logunit 10, directly beneath the gamma-ray peak, *I. multiplexum* has its LOD (D8). Another acme of *O. israelianum* (>60%) occurs higher up in the interval (D9). The amount of reworking is consistently high in the middle part of logunit 10.

The assemblages from logunit 15 to the lower part of logunit 17 (D10 to D12) are characterised by the near absence of *O. israelianum* (D10). In the lowest part of the interval, between D10 and D11, reworking is present. In the rest of the interval, from D11 to D12, the dinocyst assemblages are dominated by the sub-polar to polar *Filisphaera*/*Habibacysta* group (up to 80%; particularly *F. filisphaera* is abundant), while *Spiniferites* is common. In well B16-1 and B17-6, *A. umbracula* is present in this interval and the LOD of *A. umbracula* (D13) is recorded within logunit 17.

After dinoflagellate event D12, autochthonous dinocysts are rare to absent while fresh-water algae and reworked dinocysts are common within the upper part of logunit 17 and logunit 18.

4.3. Pollen

Pollen counts were performed in five boreholes and a composite pollen stratigraphical record of thirteen events (P1 to P 11, P3a, P4a) is described in the following according to Fig. 5 and to the Appendix. Pollen counts of trees, shrubs and terrestrial herbs were included in the pollen sum. Both trees and shrubs, including conifers such as *Pinus*, *Picea*, and *Tsuga*, are referred to as arboreal pollen in this paper. The terrestrial herbs, or non-arboreal pollen, have been divided into ericaceous dwarf shrubs (Ericales) and herbs proper. Aquatic palynomorphs, fern spores, Mesozoic and Early Tertiary pollen as well as spores and remains of non-palynomorphs were counted but excluded from the pollen sum.

High proportions of Miocene pollen types characterise the assemblages below the Mid-Miocene unconformity (MMU). At the base of the investigated interval, from logunit 1 to the base of logunit 6, the samples contain generally little pollen. Until pollen event P1, they are dominated by *Pinus* (70–80%); *Alnus* and *Picea* are consistently present as minor elements (<10%). Non-arboreal pollen makes up less than 20% of the pollen sum with Ericales only exceptionally exceeding 10% (max. 16%).

In logunit 6 to 9 (P1 to P3) the pollen assemblages remain dominated by arboreal pollen while non-arboreal types are more abundant (25–50%). *Pinus*, although still dominating among the arboreal pollen (40–60%), shows a decreasing tendency. *Alnus* and *Betula* are consistently present (<10%). The freshwater alga *Pediastrum* has its first common occurrence (FCO) (P1) and shows an increasing tendency. Although *Picea* is generally less common than in the underlying interval, there is one characteristic peak of *Picea* (P2) of 15–20%. At this level, *Tsuga* and *Osmunda* are also more common, while the non-arboreal pollen content is low (9–12%) and *Betula* is absent. Characteristic for this interval is the high proportion of Ericales (11–39%) that show an increasing tendency until P3, the top of the first Ericales acme.

In the interval from logunit 9 to 10 (P3 to P5) arboreal pollen generally dominate with 50–80% over non-arboreal pollen. *Pinus* is again the most abundant element (20–60%) while *Alnus* and *Betula* are consistently present. Although the total of non-arboreal pollen is comparable to that of the underlying unit, the assemblages are characterised by lower proportions of Ericales (<10%) and higher proportion of *Poaceae* and *Cyperaceae*. Near the gamma-ray peak of logunit 9 the first *Pediastrum* peak (P3a) is observed. At the gamma-ray low at the base of logunit 10, high numbers of *Picea* (approx. 15%) and a *Osmunda* peak (P4) are observed. Directly above the P4 level, the abundance of Ericales slightly increases (up to 20%) and a distinct peak of reworking is observed. This is followed by a peak occurrence of *Artemisia* (P4a) together with the second *Pediastrum* peak, near or at the gamma-ray peak of logunit 10. The *Pediastrum* distribution is mirrored by *Osmunda* that shows a low abundance at this level. In

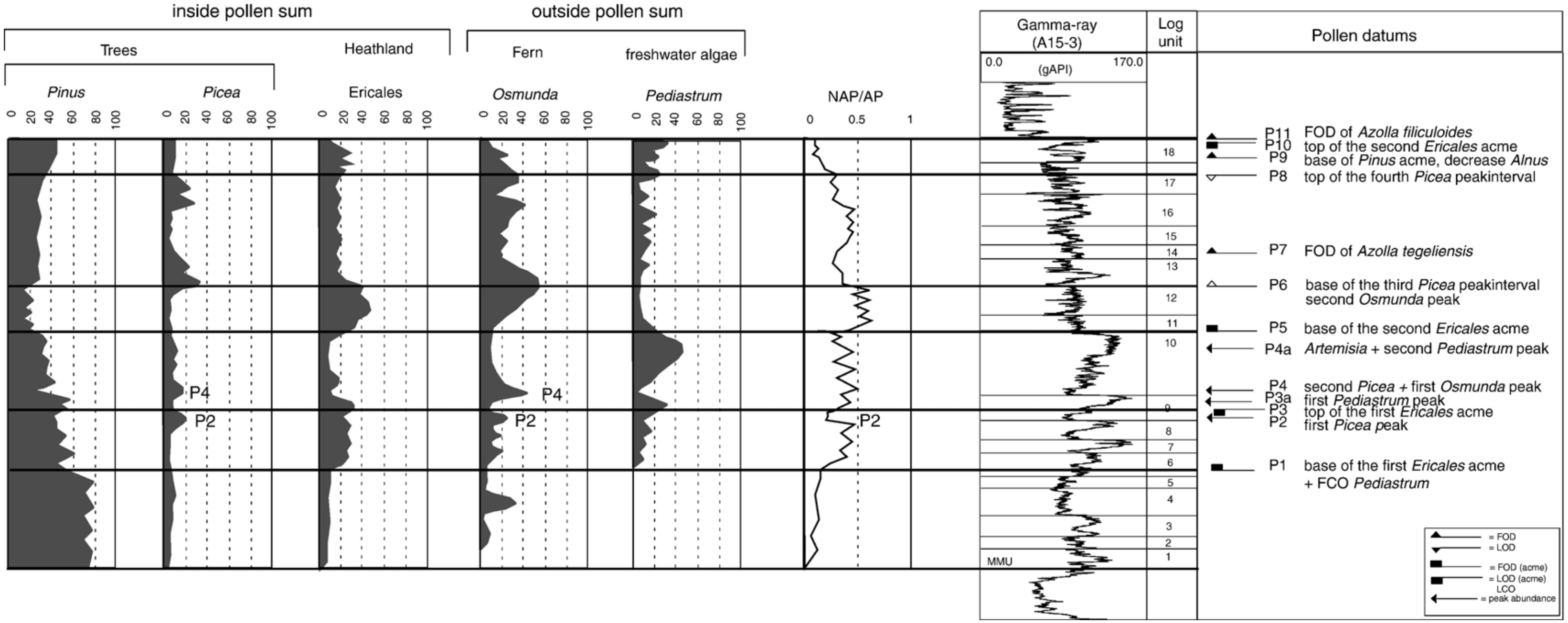

Fig. 5. Schematic diagram of the pollen results for the composite section showing the 13 most important events and their stratigraphic position related to the gamma-ray log. For explanation of abbreviations see Fig. 4.

general, the interval from P5 to P10 is characterised by high frequency changes of *Picea*, Ericales and *Osmunda*.

In the interval of logunits 11 and 12 (P5 and P6) non-arboreal pollen predominate (commonly 55–70%). Starting at the base of the second Ericales acme (P5), Ericales is present in high quantities (20 to 50%). The proportion of *Pinus* reaches minimum values (8–23%), but this genus remains the most common arboreal element together with *Alnus*. *Betula* and *Picea* are consistently present but the latter is less common than in the previous interval.

The composition of the assemblages within logunits 13 to 15 and the lower part of unit 17 (P6 to P8) is variable. The lower and upper parts of the interval are characterised by high proportions (1136%) of *Picea*; the third (P6) and fourth (P8) *Picea* peak interval, in between the percentages are low and vary between 1 and 10%. The trend of *Picea* is more or less identical to the one of *Osmunda*, which also shows distinct peaks at the base and the top of this interval. *Pinus* is the main arboreal element (up to 30%); *Alnus* and *Betula* are consistently present (< 10%). Non-arboreal pollen make up approximately half of the assemblage, but a decrease to 25% is apparent in intervals with a high *Picea* content. Ericales commonly constitute between 15% and 20% of the pollen sum. The FOD of *Azolla tegeliensis* (P7) is recorded within logunit 14. In well B17-5, arboreal pollen are more abundant than in the other wells caused by increased percentages of thermophilous trees (*Alnus*, *Carpinus*, *Quercus* and *Ulmus*.

The interval between the uppermost part of logunit 16 to logunit 17 (P8 to P11) is sampled in wells B10-3, B13-3 and A18-2 only. The composition of the assemblages varies considerably between the wells. In well B10-3, non-arboreal pollen dominate while in well B13-3, more southward, lower frequencies are recorded and in A18-2, even more southward, arboreal pollen dominate.

After the top of the fourth *Picea* peak (P8), *Picea* is only a minor constituent, mounting to not more then 5 to 10%. In all wells *Pinus* is the main arboreal element (P9) (<40%) and percentages increase towards the southwest. *Betula* is second most important among the arboreal pollen (maximum 13%), *Alnus* is only present in very low quantities. The proportion of Ericales is generally high, varying between 10 and 30%, until the top of the second Ericales acme (P10), then it is reduced to 10%. The apparent first occurrence of *Azolla filiculoides* (P11) is recorded from the upper part of logunit 18.

Samples from above logunit 18 (after P11) consist mainly of cuttings (see Fig. 3a and b) and unfortunately do not give a consistent picture of the assemblages anymore and are excluded from this research.

4.4. Foraminifera

The foraminiferal record from three boreholes (B10-3, B13-3 and B17-6) is summarised as a succession of 15 datums (Fig. 6). Some of these datums are considered to be synchronous, while others might be influenced by facies differences between the wells.

From below the MMU only a few samples were studied (Fig. 3), but the apparent LOD of the benthic species *Asterigerina staeschei* (F1) is found directly below the base of logunit 1. In cutting samples from directly above the gamma-ray peak of the MMU, *Uvigerina macrocarinata* and the nonforaminifer species *Bolboforma fragori* occur. The lower part of logunit 1 (between F1 and F2), yields well-preserved foraminiferal assemblages with common benthic species as *Bulimina aculeata*, *Elphidium excavatum*, *Loxostomum lammersi* and *Melonis affinis*. Left-coiled *Neogloboquadrina atlantica* species predominate among the planktonic foraminifers. At the boundary of logunit 1 and 2 the diversity of foraminifer species drops for a short interval.

The interval from logunit 2 to 5 (F2 to F4) is characterised by the absence of the benthic species *B. aculeata*. The benthic assemblages are diverse and are characterised by high proportions of keeled *Cassidulina* species (*carinata* and *teretis* types) with common *Cibicides* spp., *E. excavatum*, *Eponides umbonatus*, *Globocassidulina subglobosa*, *L. lammersi*, *M. affinis*, *Monspeliensina pseudotepida*, *Trifarina bradyi*, *T. angulosa*, and *Sigmoilopsis schlumbergeri*. *E. hannai* appears for the first time at the base of logunit 4 (F3) in well B17-5 and in logunit 6 in the other wells. Planktonics are abundant at the base of the interval, especially in B10-3 and B13-3, where they make up about half of the total assemblage; upwards the number of planktonics decreases at all sites. The planktic assemblages consist almost exclusively of left-coiled *N. atlantica*, occasionally *Globigerina bulloides* or right-coiled *N. atlantica* occur. The species diversity decreases rapidly over this interval. The assemblages are well preserved except in logunit 3, where dissolution of the calcitic tests is observed.

The interval from logunit 6 to 9 (comprising F4, F5, F13 and F14) is characterised by the re-introduction of the benthic species *B. aculeata* (F4) that occurs in large numbers. Planktonics, predominantly left-coiled *N. atlantica*, occur in the lower part of the interval, but they disappear from the record within logunit 6 (F5), in the overlying sediments only single specimens are found occasionally. *E. umbonatus*, *G. subglobosa* and *T. bradyi* have their last occurrence at the base of logunit 6. The species *M. pseudotepida* (F13) has its LCO within

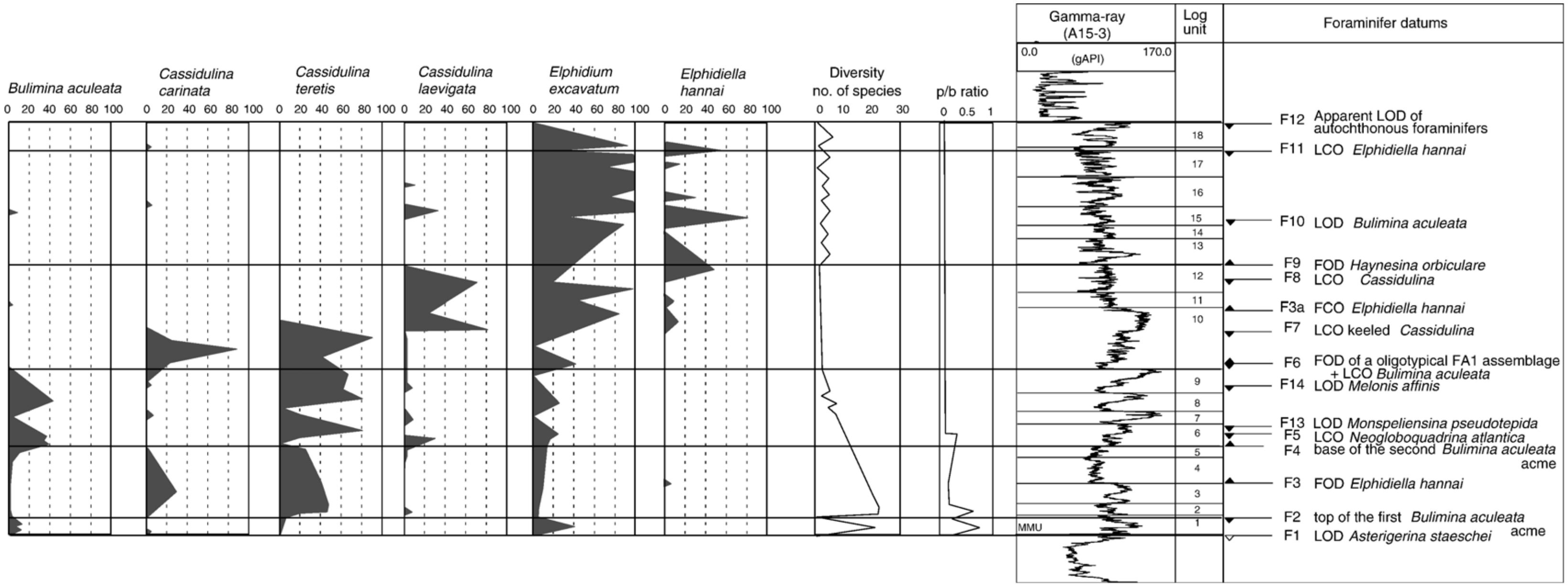

Fig. 6. Schematic diagram of the foraminiferal results for the composite section with the 15 most important events and their stratigraphic position related to the gamma-ray log. For explanation of abbreviations see Fig. 4.

logunit 6, while *M. affinis* (F14) disappears at the base of logunit 9. *Cassidulina teretis* and *B. aculeata* are common in logunit 6 to 9. Logunits 7 and 8 (only sampled in B10-3) show diverse benthic assemblages with common *B. aculeata*, keeled *Cassidulina*, *E. excavatum* and *M. affinis*. Towards the top of the interval, the predominance of *B. aculeata*, keeled *Cassidulina* and E. *excavatum* with occasionally abundant *C. laevigata* displays an upwards decreasing diversity. Many of the species common in the North Sea Basin since the Late Miocene, such as *L. lammersi*, *M. affinis* (F14), *M. pseudotepida* (F13), *S. schlumbergeri* and *Trifarina angulosa*, have their LOD in this interval. The interval from logunit 10 to 12 (F6 to F9 and F3a) is characterised by a change to low-diversity benthic assemblages dominated by either *Cassidulina* species with *E. excavatum* in the lower part or *E. excavatum* with *Elphidiella hannai* in the upper part. These low-diversity assemblages, typically made up of only two or three species, occur from this point onwards at all sites. Directly above the base of logunit 10 at the gamma-ray low, *E. excavatum* is dominant and keeled *Cassidulina* species occur abundantly below the broad gamma-ray peak of logunit 10 (F7), but become very rare in the upper part of the interval. Directly at the gamma-ray peak *C. leavigata* becomes predominant, while above the gamma-ray peak, *E. excavatum* is dominant and *E. hannai* is from then on consistently present. Towards the top of logunit 12 all *Cassidulina* species become very rare (F8) and some samples show strong dissolution. In well B17-5 one of the samples from logunit 12 yields an anomalous assemblage characterised by the common occurrence of *Virgulina fusiformis*.

The interval between logunits 13 and 17 (F9 to F11) is characterised by the intermittent presence of *Haynesina orbiculare*. From foraminifer event F9 onwards low-diversity assemblages, similar to those in the underlying interval, occur at all sites. Samples from intervals with high and intermediate gamma-ray values are often barren. The assemblages are generally dominated by *E. excavatum* or, in gamma-ray lows, by *E. hannai*. *Cassidulina* occurs at two distinct levels, the first occurrence is at the boundary between logunit 15 and 16 with common *C. laevigata* (30–40%), and the second is in logunit 16, where *Cassidulina* is much less common. The assemblage from the first level is further characterised by *B. aculeata* (ca. 7%). This is the only interval above the top of logunit 9 in which *B. aculeata* exceeds 5% and it is taken as the LOD of *B. aculeata* (F10). In logunit 17 *E. bartletti* is found in B17-05. The LCO of *E. hannai* (F11) is observed at the top of logunit 17.

The samples close to the base of logunit 18 (F11-F12) are barren. In this logunit either *E. excavatum* or *H. orbiculare* dominates low-diversity assemblages. *Elphidium ustulatum* is common in some samples. The sediments directly overlying unit 18 contain allochthonous foraminifers that are not included in further interpretations.

4.5. Paleomagnetism

The paleomagnetic results of the discrete measurements on core and sidewall core samples are shortly described before an integrated interpretation of the measurements with the Geological High-resolution Magnetic Tool (GHMT) is given (Fig. 7a).

Core samples taken for paleomagnetic analyses from well A15-3, consist mainly of silty to clayey sediments that are suitable for recording a reliable paleomagnetic signal. A small viscous component is in all cases removed between 100 to 150 °C. The component removed at temperatures between 210 and 280 to 300 °C has been taken for interpretation. At a maximum temperature of 390 to 420 °C the characteristic remanent magnetisation (ChRM) is entirely removed. In general, the direction of the ChRM could be straightforwardly derived from a linear decay towards the origin of the Zijderveldplot. Within the middle part of the borehole (logunits 8 to 10), an interval of consistently normal polarities exists between 920 and 936 m (right column of Fig. 7a). Above and below that interval reversed polarities are recorded. Core samples of the upper part of the borehole (logunit 15) all show reversed polarities. Only one sample at 621 m yielded normal polarity, most likely caused by late diagenetic processes, since it occurs within an oxidised layer; therefore this level is discarded as representing true normal polarity.

The ChRMs of the sidewall core samples were derived from alternating field (AF) as well as thermal demagnetisation. Both demagnetisation methods show unreliable magnetic behaviour of the sidewall cores. These samples had a strong overprint of the present day field, probably caused by storage conditions. However, reliable interpretation was possible for 18 samples. When using AF demagnetisation, the samples often acquire a gyroremanent magnetisation at fields between 40 and 70 mT. During thermal demagnetisation, the present day field overprint is removed only at temperatures up to 300 °C, therefore datapoints from higher temperature ranges, between 330 and 510 °C, had to be interpreted. Unfortunately, most of the remanent magnetisation is already removed at these temperatures, as shown for the core samples. Thus, ChRM results obtained from thermal demagnetisation are less reliable then those derived from AF demagnetisation. The obtained polarities are plotted per sidewall core sample in Fig. 7.

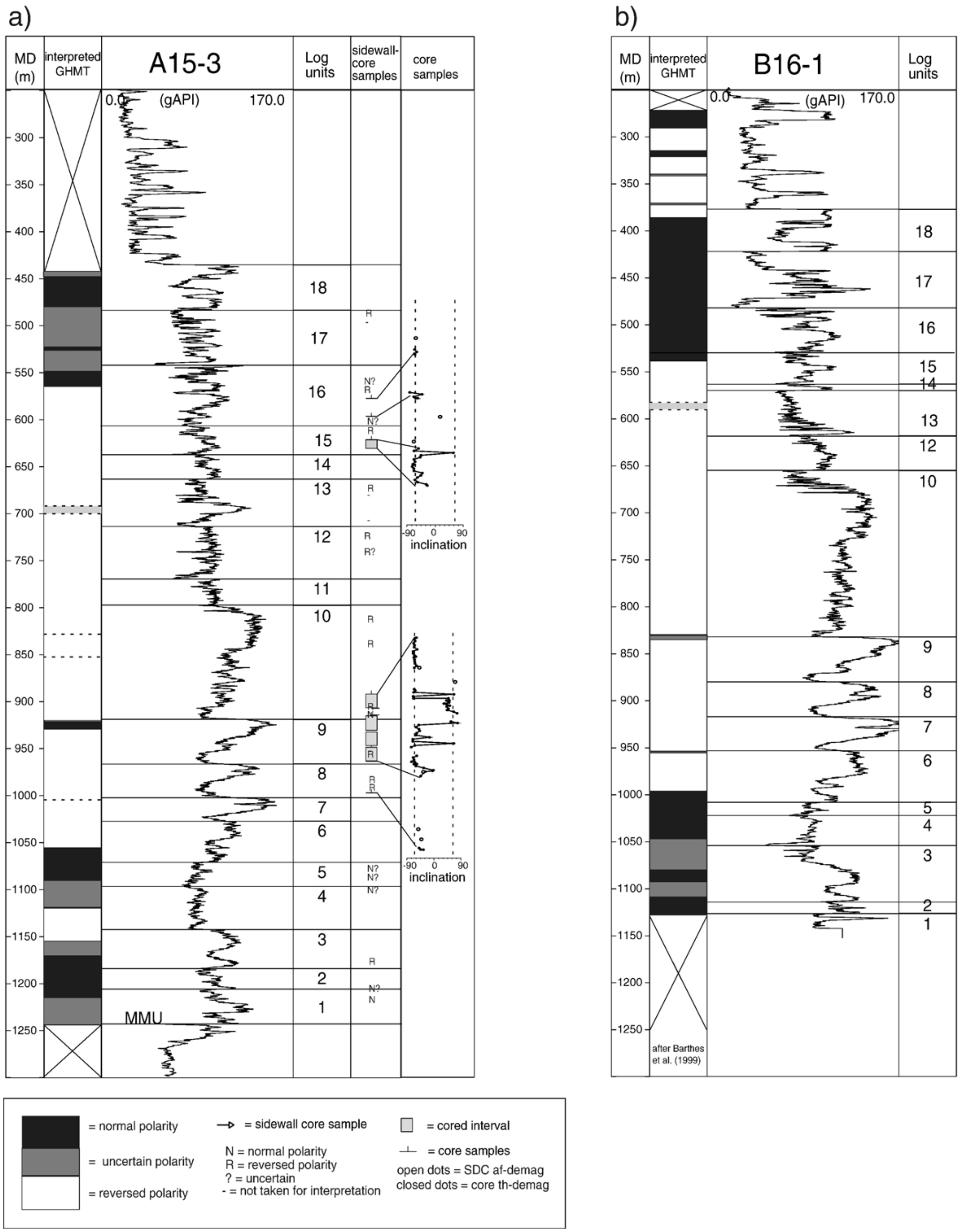

Fig. 7. a) Inclination results from sidewall-core and core samples from well A15-3, right panel, and integrated paleomagnetic interpretations of well A15-03, left panel — b) Polarity interpretations of well B16-01 (after Barthés et al., 1999).

The GHMT interpretation was made by Schlumberger, Paris, applying a method very sensitive to the centring of the susceptometer tool in the borehole. Usually, data processing is used assuming the tool is not centred. This assumption maximises the induced component, in this particular case the reversed polarity zones.

Conversely, assuming the tool as centred minimises the induced component and the obtained results show that in our record most of the earlier uncertain zones appear as consistent normal polarity zones. In our case the normal polarity zones, of which one is clearly confirmed in the core samples, are better defined in the GHMT interpretation by processing the data according to the latter assumption.

Fig. 7 (left column) shows the compiled results of the reprocessed GHMT data set, with the integrated results of the discrete sample of the well A15-3. The interpretation of the geomagnetic record is done in terms of normal, reversed and uncertain polarity intervals. Normal polarity intervals are interpreted in the lower part of the succession (logunit 1 to 6) between 1214 to 1170 and 1090 to 1056 m depth. There is a predominantly normal interval from 565 to 448 m (logunits 15 to 18) in the upper part of the section. The entire interval between 1056 and 565 m shows reversed polarity, except for one short normal and several uncertain polarity intervals. This normal polarity occurs between 929 and 920 m depth (logunit 9). Three of the uncertain intervals are not more than one metre thick, but there is one fourteen metre thick interval between 691 and 705 m depth.

5. Interpretation and discussion

5.1. Integrated chronostratigraphy

All biostratigraphic data from the eight boreholes have been integrated and will be discussed in combination with the derived paleomagnetic record.

Below the Mid-Miocene Unconformity or MMU, the sediments of the investigated succession in the southern North Sea (Fig. 1) can be dated as Middle Miocene or older, on basis of the foraminifer *A. staeschei* (F1) (Doppert et al., 1979; King, 1983). Also the dinoflagellate species *A. spiridoides*, *P. ventricosum* and *U. aquaeductum* below the MMU indicate a Middle Serravallian age, approximately 12 Ma, (Middle Miocene) or older (De Verteuil and Norris, 1996). Directly above the gamma-ray peak of the MMU, at the base of logunit 1, *U. macrocarinata* and *B. fragori* point to Middle to Late Miocene age (Fig. 8; Von Daniels, 1986; Spiegler and von Daniels, 1991; Spiegler, 1999). Because of the condensed character of the sediments directly above the MMU it is not possible from our data set to determine the ages for this interval with more accuracy. The onset of sedimentation onto the MMU is estimated at 12.4 Ma by Michelsen et al. (1998) for the Danish sector and at 10.7 Ma in the German sector (Streif, 1996). In the southern Norwegian sector the top of the unconformity is dated at 11.2 Ma (Eidvin et al., 1999).

The upper part of logunit 2 can be attributed to the Zanclean (Early Pliocene) through the occurrence of the dinoflagellate *R. actinocoronata*. The Zanclean–Piacenzian boundary dated at 3.6 Ma (Castradori et al., 1998) is placed at the level of the D1 event (Last Occurrence Datum — LOD *M. choanophorum*), at the base of logunit 3 (Fig. 4). The appearance of *E. hannai* (F3) is taken as indicator of the foraminiferal FA zone (Doppert, 1980) and NSB 14 zone (King, 1983) supporting a late Early to early Late Pliocene age for the interval from logunit 4 upwards. The disappearance of *Barssidinium* spp. (D2) and the first occurrence of *I. multiplexum* at the upper boundary of logunit 5 (Fig. 4) suggest both a Piacenzian age (Fig. 2). This datum is located just below the top of a normal polarity interval. Together with the occurrence of left coiled *N. atlantica* (F5) below logunit 6, the underlying sediments predate 2.4 Ma, since that is the LOD of this species in the Atlantic region (Weaver and Clement, 1986; Spiegler and Jansen, 1989). In the Mediterranean *N. atlantica* has its LOD in marine oxygen isotope stage (MIS) 96 (Zachariasse et al., 1990). As a consequence, the polarity boundary found at a depth of 1056 m in A15-3 and at 996 m in B16-1 (Fig. 7b) can only be interpreted as the Gauss–Matuyama (G–M) boundary, with an age of 2.582 Ma (Lourens et al., 1996). An important consequence of this interpretation is that the provisional LOD of the dinoflagellate *B. minuta* and *A. andalousiensis suttonensis*, defined by Head (1998) in the North Sea Basin near the base of the Gauss Chron, must now be shifted towards the top of the Gauss Chron, at the level of dinoflagellate datum D2.

The interval below the G–M boundary is highly condensed and an unambiguous interpretation of the paleomagnetic pattern below this level is not possible. Above the G–M boundary until the top of logunit 15, the long interval of reversed polarity is interpreted as belonging to the Matuyama Chron. The consistent presence of *A. umbracula* from logunit 6 upwards, and in particular its disappearance in logunit 16 (D13), places the whole interval within the Gelasian (Late Pliocene) (Fig. 2; De Vernal et al., 1992).

At the top of the investigated succession, the occurrence of *A. filiculoides* (P11) (Fig. 5) marks the Tiglian C5 north-west European regional stratigraphical stage (Zagwijn, 1963; Gibbard et al., 1991). This stage encompasses the upper boundary of the Olduvai subchron that is found within the continental record of northern Belgium (Kasse, 1996) and south-east England (Hallam and Maher, 1994). The lower boundary of the Olduvai subchron, dated at 1.942 Ma (Lourens et al., 1996), is

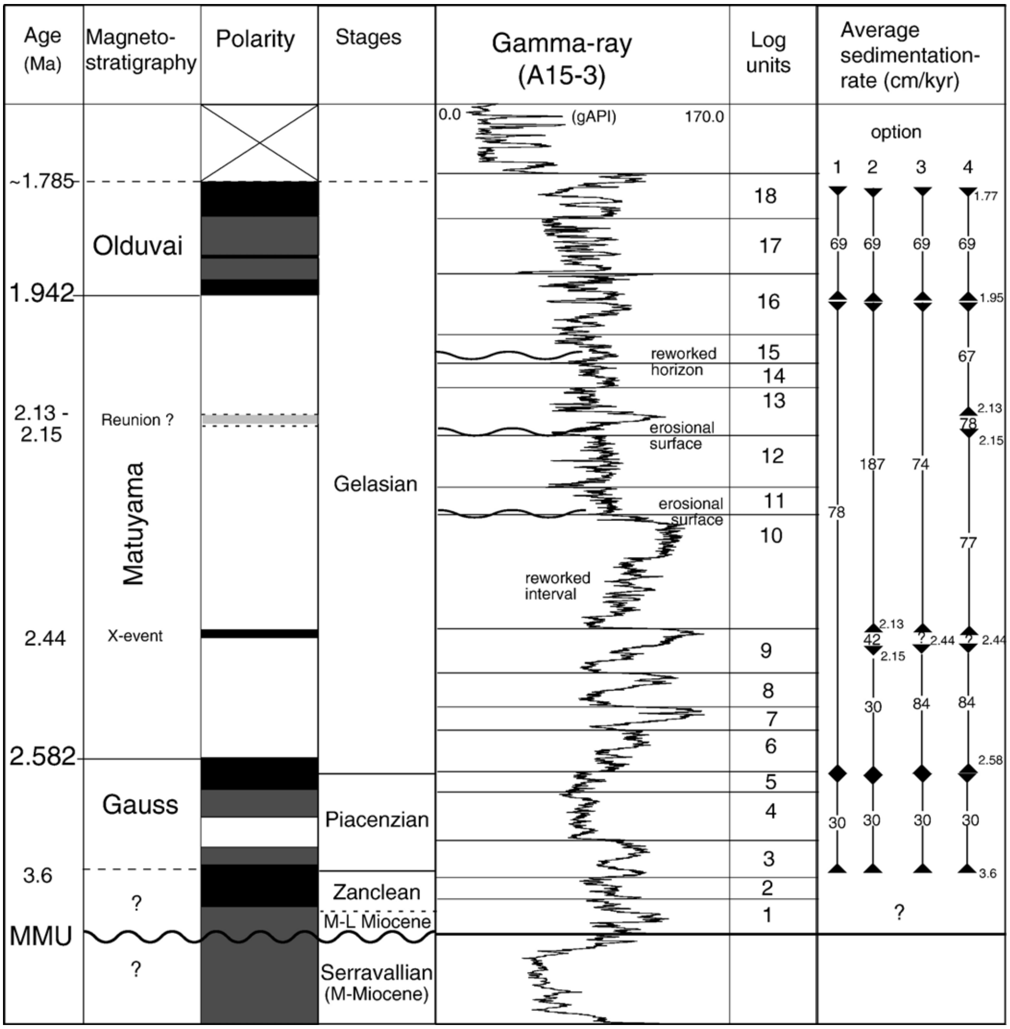

Fig. 8. Integrated bio- and magnetostratigraphic chart, related to the logunits with respect to the standard chronostratigraphy. The right panel shows the four options for sedimentation rates. Note that the vertical scale is linear in metres, not in age.

recorded at 564.5 m in A15-3 in the upper part of logunit 15, and at 538 m in B16-1 in the middle of logunit 15 (Fig. 7a and b). Although the upper boundary of the Olduvai is probably not reached in well A15-3 by the measurements, it has been extrapolated to a depth of 441 m by carefully correlating the gamma-ray log to that of B16-1 where this boundary is recorded at 368 m (Barthés et al., 1999). Hence, logunits 15 to 17 comprise the Olduvai subchron.

From the above data it can be concluded that increased sedimentation rates in the studied area started no earlier than the Late Pliocene, at the Zanclean–Piacenzian boundary, and continued until the Pliocene–Pleistocene boundary near the top of the Olduvai subchron. Hence, the main part of the investigated succession at the studied location comprises the entire Upper Pliocene time interval between 3.6 and 1.8 Ma.

5.2. Short paleomagnetic events

In paleomagnetic records of North Sea sediments, several short intervals of normal polarity have been described between the Olduvai subchron and Gauss chron (Fig. 7; Cameron et al., 1984; Streif, 1996; Barthés et al., 1999). Since the occurrence of short paleomagnetic events may help to date the sediments more precisely and, as a consequence, may lead to more accurate estimates of sedimentation rate we will discuss possible interpretations of the short normal polarity zones within the Matuyama Chron.

At the top of logunit 9, the nine metre thick normal polarity interval of A15-3 at 929–920 m can directly be correlated to a normal but less certain interval in B16-1 (Fig. 7b) which has been interpreted as the Reunion subchron by Barthés et al. (1999). They refer to a second interval in B16-1, between 954 and 955 m, as Reunion 2, whereas another uncertain interval between 565 and 580 m within logunit 13 has not been discussed at all. This latter interval, however, can be correlated to a similar uncertain interval in well A15-3 occurring within logunit 13.

On seafloor spreading profiles, Cande and Kent (1992) describe two paleomagnetic anomalies between seafloor anomalies 2 (Olduvai) and 2A (Gauss), of which the younger one corresponds to the Reunion subchron (Grommé and Hay, 1979) and the older one corresponds to the X-anomaly (Heirtzler et al., 1968). This 'X-event' was observed in magnetic anomaly profiles with high spreading rate (Blakely and Cox, 1972; Rea and Blakely, 1975), but until now this event has not been confirmed by any magnetostratigraphic evidence in sedimentary sections. Here, we discuss two possibilities to link the North Sea anomalies from our dataset to the global scale. The first possibility implies that the short normal interval within logunit 9 is the Reunion subchron, with an astronomically calibrated age of 2.13 to 2.15 Ma (Lourens et al., 1996). The second possibility interprets this normal interval as the X-event or the Cryptochron C2r.2r-1 that has been dated by Cande and Kent (1995) from 2.42 to 2.441 Ma. In the latter case, the upper uncertain interval within logunit 13 could then represent the Reunion subchron.

These two possibilities result in four different options for the sedimentation rates calculated for well A15-3. These options are displayed in Fig. 8 and discussed in the following. Fig. 9 shows the correlation of our paleomagnetic interpretation to the oxygene isotope curve by Tiedemann et al. (1994) and corresponding global marine isotope stages. The simplest option (option 1 in Fig. 8) involves calculation of the mean sedimentation rate from the G–M boundary to the base of the Olduvai, resulting in an overall average value of 78 cm/kyr, not taking any paleomagnetic events or breaks in sedimentation into account (see Fig. 8). Below the G–M boundary a sedimentation rate of 30 cm/kyr is calculated based on the age of the Zanclean–Piacenzian boundary. If we assume that the normal event within logunit 9 is the Reunion (option 2), the sedimentation rate would be 30 cm/kyr for the interval above the G–M boundary (Fig. 8). Such a low rate for the interval below the normal event seems unlikely for this part of the succession, since by that time the depocentre was located in the studied area (Fig. 10, and Kuhlmann, 2004). This would imply higher sedimentation rates for this interval than for the lower, condensed part of the succession. Furthermore, this option would imply an average sedimentation rate of 187 cm/kyr for the upper part of the succession. An average sedimentation rate up to 187 cm/kyr seems too high for the interval above the normal event, as such high rates are found in turbiditic and equivalent mass flow environments. On the basis of well-log profiles (Fig. 3a and b), from biostratigraphic evidence as well as from 2D and 3D-seismic data (Kuhlmann, 2004), at least two erosional surfaces and one reworked horizon can be observed for this part of the succession (Fig. 8). This suggests that sedimentation rates must have been even higher if the eroded material is taken into account. We therefore believe that option 2, i.e. interpreting the lower short normal event as the Reunion subchron, is not realistic for this environmental setting.

In option 3, the normal polarity event within logunit 9 corresponds to the X-event. In this case, average sedimentation rates are respectively 84 cm/kyr between the G–M boundary and the X-event, and 74 cm/kyr between the X-event and the lower Olduvai, taking a midpoint of 2.43 Ma for the X-event (Cande and Kent, 1995). These sedimentation rates are consistent with the environmental setting, where an increase of sedimentation is expected around logunits 5 to 6. It is logical to expect that sedimentation is relatively continuous up to logunit 10, with a steadily increasing sedimentation rate, since the depocentre approaches the studied wells (Kuhlmann, 2004). From logunit 11 onwards, the progradational bodies have moved further west. Another strong indication for the X-event is its position at what we interpreted as top of isotope stage 96 (see Section 5.3.4.2 and Kuhlmann, 2004). This position prohibits the Reunion, since that correlates with isotope stage 81 (Lourens et al., 1996). Finally, in our option 4 (Fig. 8), we propose that the Reunion is represented by the uncertain polarity interval just above 700 m in logunit 13. Although there is a greater chance in observing the Reunion subchron than the X-event because of its longer duration, the Reunion seems to be more uncertain in our case because of its location near an erosional surface (Fig. 8). In option 4, the average sedimentation rate between Reunion and lower Olduvai is 67 cm/kyr, which is consistent with the average sedimentation rate below the Reunion (77 cm/kyr) and the (minimum) sedimentation rate in the Olduvai subchron (69 cm/kyr) (Fig. 8).

The presence of the X-event in the sediments of the North Sea Basin is in accordance with our new interpretation of the results of Barthés et al. (1999), where a short interval with normal interval was recorded at the same stratigraphic position. Our interpretation agrees furthermore with two short normal polarity intervals found in the Westkappelleground Formation (Cameron et

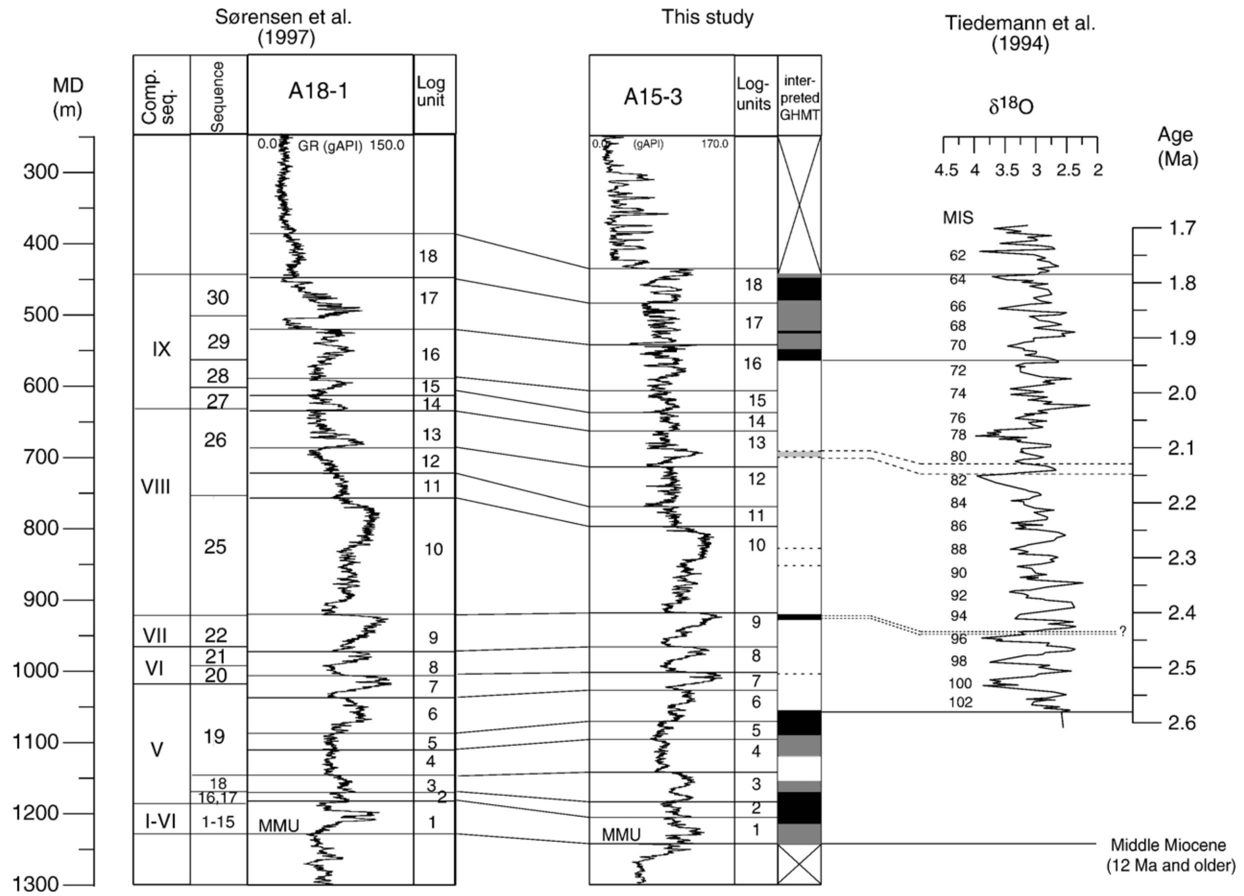

Fig. 9. Gamma-ray curve from the reference well of this study (A15-3) with its logunits and paleomagnetic polarities correlated to the sequences by Sørensen et al. (1997) and to the oxygen isotope curve with the corresponding marine isotope stages (MIS) by Tiedemann et al. (1994) as inferred by the paleomagnetic boundaries.

al., 1984). They tentatively interpreted these normal events as Reunion subchron and X-event, although this interpretation could not be substantiated by a robust chronostratigraphy. Here, we propose to introduce the name 'North Sea event' for the hitherto unnamed 'X-event'. Nevertheless, more detailed investigations elsewhere are necessary to authenticate this geomagnetic event, either as a reversal excursion or a true subchron.

5.3. Paleoclimatological and -environmental interpretations

The three investigated fossil groups not only provide stratigraphical data but also important information about the paleoenvironmental evolution of the North Sea region during the Late Pliocene. In the following the combined results of dinocysts, pollen and foraminifers (Figs. 4–6) are discussed and integrated in Fig. 11.

5.3.1. Dinoflagellate cysts

Dinocyst distribution is mainly controlled by four environmental parameters:

(1) The Sea Surface Temperature (SST) or climatic signal; to avoid confusing terminology as 'warm' and 'cool, the classification of Dale (1996) is used. In his actualistic classification, four biogeographic zones were distinguished: Polar, Sub-polar, Temperate and Equatorial.
(2) The coastal/oceanic signal; in line with most dinocyst workers, four main categories are distinguished in the marine realm: restricted marine (estuarine, lagoonal or coastal), inner neritic, outer neritic and oceanic.
(3) The salinity signal; because of the complexity of the salinity signal (e.g. intra-specific morphological variation), only reduced salinity or freshwater influence is mentioned in this study.

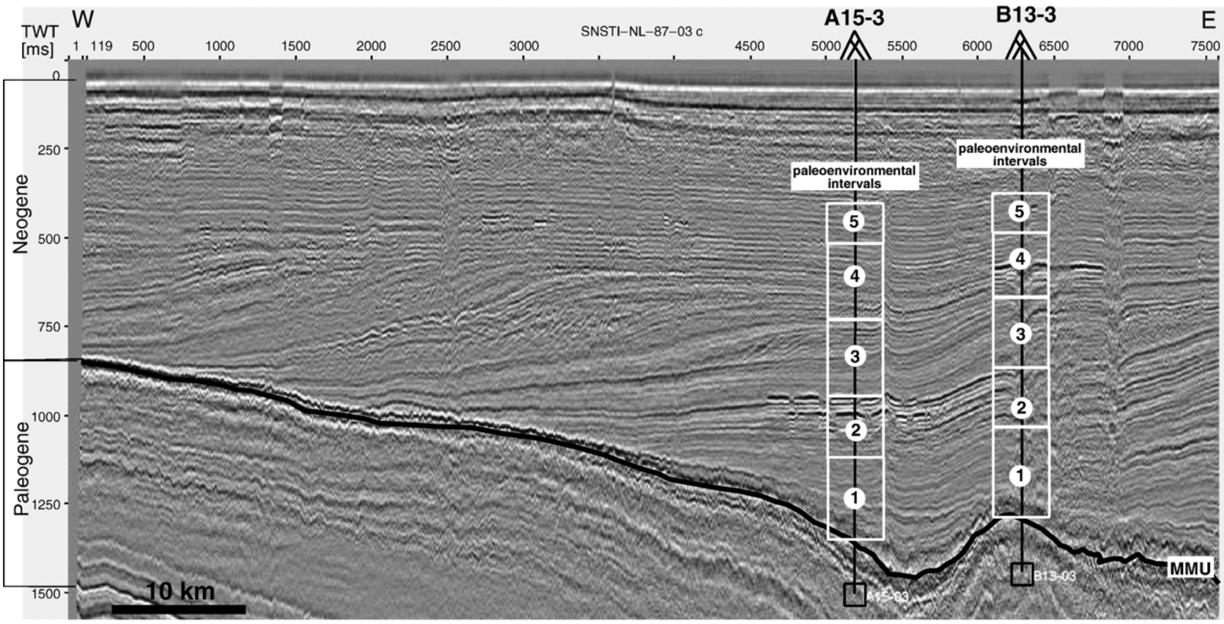

Fig. 10. Seismic profile modified from Kuhlmann (2004), showing the progradational environment above the Mid-Miocene Unconformity (MMU) and the inferred paleoenvironmental intervals for two boreholes (A15-3, B13-3). The location of the seismic profile is given in Fig. 1.

(4) The productivity signal; enhanced productivity may result from increased run-off, it occurs in upwelling settings or from melting sea-ice in glaciomarine environments.

If not otherwise stated, we refer to Edwards and Andrle (1992), Dale (1996) and De Vernal et al. (2001) for details on dinocyst ecology.

5.3.2. Pollen and spores

In marine sediments pollen and spores are allochthonous components. In our interpretation, we presume that the majority of the pollen and spores are primarily transported by rivers rather than by wind because a huge river supply dominated the sedimentary composition. The assemblages are thus assumed to represent a mixture from the fluvial drainage area. Because the Late Pliocene sedimentation in the North Sea was dominated by the Baltic river system (Gibbard, 1988), a significant proportion of the pollen assemblages is expected to represent a signal from both areas at high latitudes and from far inland the European continent. In contrast, Pliocene–Pleistocene deposits from the southern onshore areas were part of the Rhine and Meuse river system which include significant pollen from thermophilous trees like *Alnus*, *Quercus*, *Carpinus* (Zagwijn, 1963). Our record shows a relatively low abundance of pollen from southern source areas and pollen of warm temperate elements, typical of Early Pliocene forests, such as *Nyssa*, *Sciadopitys*, *Sequoia* and *Taxodium* type pollen are of low relevance in our record. This can becaused by the northern position and thus cooler signal from the drainage area or may reflect the general climate-related shift of pollen assemblages during the Late Pliocene. Another characteristic in our record is the overall high percentage of *Pinus* which may be overrepresented in marine sediments because of its high buoyancy (Traverse, 1988). Nevertheless, a (climate-) stratigraphical interpretation of the pollen assemblages is possible by looking at the relative changes of the most important components in the assemblages. Thus, stratigraphic interpretation in terms of climate changes is based on the following assumptions:

(1) Relatively cold climate: high abundances of Ericales and *Artemisia*, both indicating open vegetation of the hinterland.
(2) A relatively warm climate: high abundance of *Picea* and the spores of temperate brook forest understory ferns *Osmunda* and *Dryopteris*.
(3) For additional ecological information the freshwater algae *Pediastrum*, the herb *Artemisia* as well as reworked Miocene components appear to be useful for the paleoenvironmental interpretation.

5.3.3. Foraminifera

The foraminiferal data has been used to interpret water depth, distance from the shore line and climate

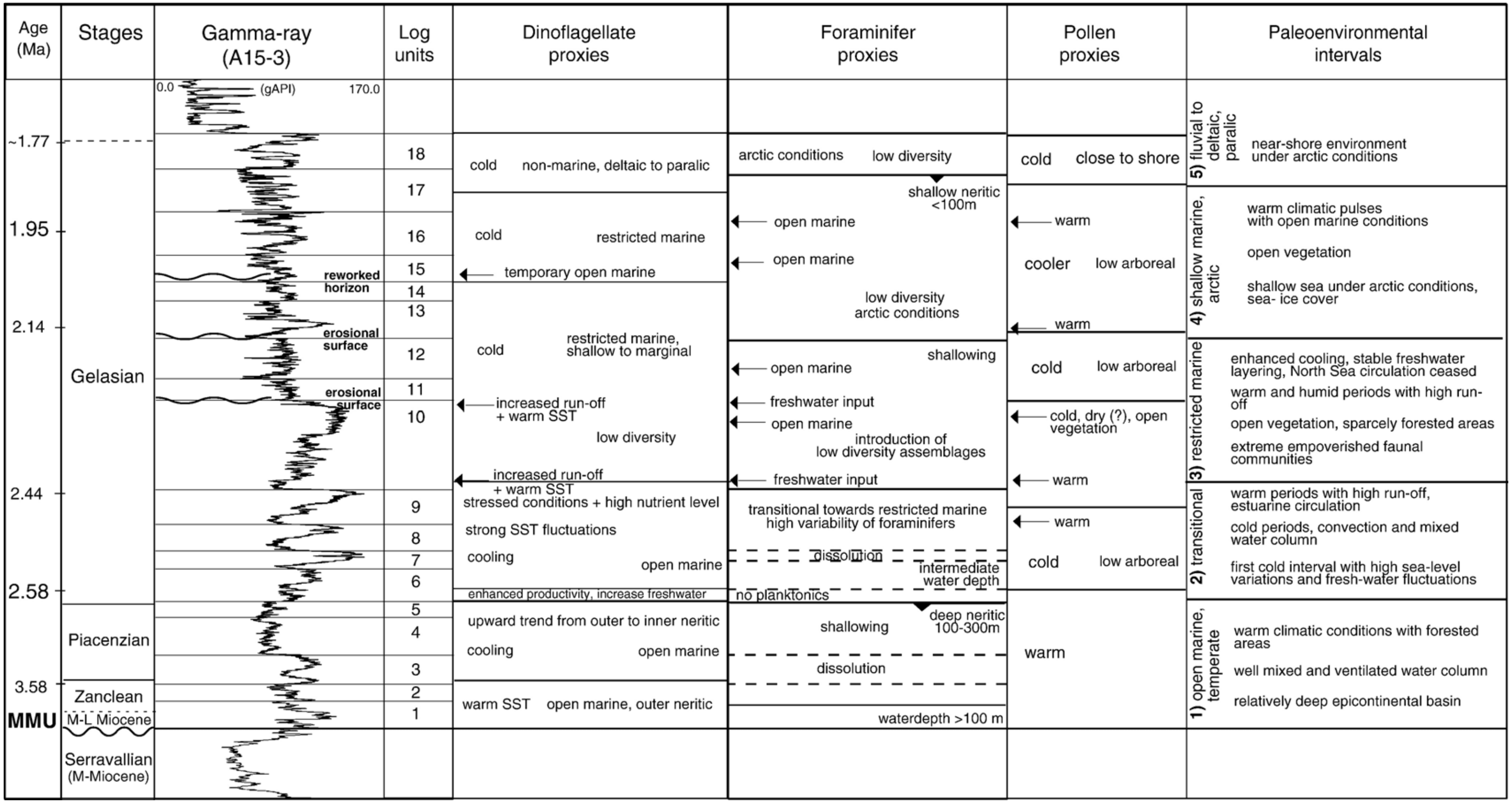

Fig. 11. Integrated environmental interpretation of dinoflagellates, foraminifers and pollen, related to the log units. The resulting five paleoenvironmental intervals are indicated on the right.

conditions. We use the model of Gradstein and Backstrøm (1996) who distinguished five depositional environments of which the following three can be applied to our data:

(1) Deep neritic (100–200 m); with foraminiferal assemblages of varying diversity and locally common planktonics.
(2) Shallow neritic (<100 m); with foraminiferal assemblages of low generic and species diversity.
(3) Non-marine, terrestrial; with spore–pollen assemblages but no foraminifers.

From this division, a general trend evolves that benthic foraminiferal diversity increases basinward, from shallower to deeper marine conditions. Using this zonation, the most important species in our record, i.e. *C. teretis*/*laevigata*, *Ammonia* spp. and *Elphidium* spp. point to a habitat between deeper neritic (>200 m) to lower neritic (100 m). *E. hannai* occurs in shallow environments. *E. excavatum* is interpreted as a generalistic species. Further ecological interpretations are taken from Murray (1991), e.g. dependency on substrate, salinity or temperature.

5.3.4. Paleoenvironmental interpretation

In addition to a more continuous trend, five paleoecological and -environmental intervals have been distinguished within the Miocene to Pliocene North Sea record. First, the general trends in terms of sea level and (sea-surface) temperature variations will be shortly described. Then, the identification of these five paleoenvironmental intervals based on shifts in faunal and floral assemblages (Fig. 11) is discussed in more detail.

After the break in sedimentation at the MMU, the foraminifer as well as the dinocyst assemblages display a general shallowing upward trend over the entire succession from a deep neritic (100–200 m) towards a shallow neritic (<100 m) and finally non-marine setting (Fig. 11). Such a trend is also apparent by the decreasing gamma-ray values and is seen in the coarsening upward of the grain-size distribution.

The sea surface temperatures (SSTs) in the lower part of the succession were relatively high. In the overlying interval a shift towards cooler conditions has been observed and an overall cooling towards glacial conditions, either gradual or punctuated is evident from the palynological and the foraminiferal record. In accordance to our chronostratigraphy, the investigated sediments include the onset of Northern Hemisphere Glaciation around 2.6 Ma (Wolf and Thiede, 1991; Raymo and Ruddiman, 1992; Wolf-Welling et al., 1996; Thiede et al., 1998; Maslin et al., 1998) and the subsequent intensification of the glacial conditions.

Hence, the lower part of investigated sedimentary record covers Middle Miocene to Lower Pliocene strata that were deposited in an open marine relatively deep setting under moderate to warm climatic conditions. Hereafter, the Upper Pliocene sediments picture the global cooling and the contemporaneous sea level lowering (Haq et al., 1987). This climate deterioration and sea level lowering forced the sediments to prograde and to fill up the marine basin. Prograding wedges were a common feature for this time interval and have been observed in the North Sea region (Gregersen, 1997; Sørensen et al., 1997), along the entire continental slope of western Norway (Henriksen and Vorren, 1996; Eidvin et al., 1999; Evans et al., 2000) as well as along the western coast of Ireland and Britain (Stoker et al., 2002) and in a global perspective (Peizhnen et al., 2001).

5.3.4.1. Open marine, temperate (logunit 1–5). The first interval ranges from the MMU to logunit 5. The pollen signal (pre P1) implies an overall warm climate based on generally high amounts of Pliocene elements and thermophilous trees, low amounts of Ericales and herbs and a low NAP/AP ratio. The dinoflagellate assemblages of logunits 1 and 2 (pre D1) with the common occurrence of *O. eirikianum* are indicative for equatorial to temperate SSTs and outer neritic, open marine conditions. During logunit 1 the foraminiferal distribution points to a water depth that exceeded 100 m. At high gamma-ray values in logunits 1 and 3, only few poorly preserved foraminifers are present which has been attributed to carbonate dissolution because of more dissolved CO2 in pore-waters or the water column. Within logunits 3 to 5 (D1–D2), the dominance of dinocysts, their high diversity and the common occurrence of the dinoflagellate species *A. umbracula* indicate that open marine conditions persisted throughout the entire interval. However, the wells B17-6 and B17-5 were probably located in a shallower environment since the first occurrence of *E. hannai* (F3) is earlier, logunit 4, in these wells whereas it appears later (logunit 6) in wells B10-3 and B13-3.

Towards the top of the first interval, the decreasing number of *Spiniferites* and the disappearance of *Nematosphaeropsis* suggest a shift from outer to inner neritic conditions. This shift may be related with a cooling of the surface waters, seen in the increase of *B. tepikiense*. The disappearance of the low latitude taxon *T. pellitum* supports the trend towards more temperate SST, which is also in line with the increase of the sub-polar to polar taxa

Filisphaera and *Habibacysta*. Furthermore, the many extinction datums near, or at the top of the interval, are probably related to a change in SST. On land, the decrease in Pliocene elements and the increasing NAP/AP ratio confirm the cooling trend over this interval.

Hence, during deposition of the basal part of the succession the North Sea Basin was part of an open marine epicontinental basin with a generally well-mixed and ventilated water column. Only exceptionally, during the deposition of fine-grained sediments stagnant conditions or high nutrient supply may have occurred. Towards the top of this interval first indications of cooling and shallowing are seen which become more prominent in the following interval.

5.3.4.2. Transitional (logunit 6–base logunit 10). The second interval is transitional between the under- and overlying intervals with respect to SST changes and the associated sea-level fluctuations. At the boundary from logunit 5 to 6, the climate conditions change from a warm climate with highly diverse faunas to the onset of colder conditions. One indication for the transition towards a colder land climate is given by the relatively high proportion of Ericales (P1–P3). At the same time the dominance of the (sub-) polar *Filisphaera*/*Habibacysta* group (D3 to D4) records a pronounced cooling of the surface water. In the lower part of logunit 6, the acme of *L. machaerophorum* (D2–D3) points to a significant increase in the availability of nutrients in the euphotic zone. This may be related to an increase in terrestrial input through higher river supply. High variations in freshwater run-off and high-frequency sea-level changes became important during this interval as seen by the GR high frequency variations. The dinocyst assemblages still reflect open marine conditions, albeit inner neritic rather than outer neritic. The termination of planktonic foraminifers in logunit 6 supports the general shallowing of the environment.

Conspicuous features of the transitional phase are high variability of the gamma-ray signal as well as of the dinoflagellate, pollen and the foraminiferal distributions. At intervals with low gamma-ray values (i.e. at the bases of logunits 9 and 10) high proportions of *Picea* and *Osmunda* (P2 and P4) and the near-absence of the *Filisphaera* Group as well as dinoflagellate events D5 and D7 indicate higher SST (temperate) and land temperatures for these levels. The diversity of the dinocyst assemblages suggests relatively high sea level. Also the occurrence of *Cassidulina laevigata* which is more frequently found in the northern part of the recent North Sea with a good connection to Atlantic surface water (Murray, 1991) points to a good connection to the Atlantic. The peak occurrence of *L. machaerophorum* indicates concomitant low salinity and high nutrient levels that can only be caused by high river run-off. On the one hand, one would expect a strong stratification of the upper part of the water column caused by a stable freshwater layer. However, on the other hand the coarser grained sediments of these periods imply a higher energetic hydrodynamic regime. Furthermore, these intervals are dominated by the foraminifer *E. excavatum* that tolerates extreme environments such as low salinity, turbid water and low food supply. Therefore, an estuarine circulation model is proposed for the North Sea during these warmer periods. This would consist of a low-saline surface water outflow and strong bottom currents that probably were fed by inflowing Atlantic water. 3D seismic amplitude maps of this periods showing elongated erosional structures confirm the finding of bottom currents (Kuhlmann, 2004). Phases of intensified along-slope currents at the northwest European margin during the Cenozoic have been reported by Laberg et al. (2005) and contourites found in older North Sea sediments were described by Huuse and Clausen (2001).

At the gamma-ray peaks, the dominance of Ericales and the *Filisphaera* group indicates cold conditions for these periods. At these times finer grained silty clays were deposited. The foraminifers show *C. teretis* peak occurrences but the individuals are general poorly preserved (i.e. at the gamma-ray peak in logunit 7). However, *C. teretis*-dominated assemblages were found in sediments deposited during glacial conditions at the Last Glacial Maximum in the Iceland–Scotland Ridge region, an area closely connected to the North Sea (Rasmussen et al., 2002), supporting our interpretation of cold conditions. During these cold intervals, the sea level must have been generally lower and we assume that the surface circulation in the North Sea was weak and possibly convection through cooling persisted which resulted in a mixed water column. The deposition of fine-grained sediments confirms the rather calm hydrodynamic conditions. 3D seismic amplitude maps of this periods confirm this finding by rather uniform seismic character (Kuhlmann, 2004).

The fossil record at the gamma-ray peak of logunit 9, however, differs from those at the underlying gamma-ray peaks, because of the near-absence of the *Filisphaera*/*Habibacysta* group (D4 to D7). Surface water temperatures must therefore have been higher than in the underlying cold periods. The diversity of both, dinocysts and foraminifers decreases in this upper part, marking the transition from an open to a shallow, marginal marine, environment. The impoverished dinocyst assemblages dominated by 'round browns' and reworked specimens in logunit 9 suggest stressed conditions, unfavourable for autotrophic dinoflagellates. The dominance of 'round browns' point to very high nutrient levels which is characteristic for glaciomarine conditions.

We conclude that during the second interval, cold climatic conditions prevailed but that the North Sea was periodically influenced by warm climatic periods. Since the G–M boundary in logunit 6 can be coupled to marine isotope stage (MIS) 103 (Lourens et al., 1996), and the gamma-ray variations of logunits 7, 8 and 9 match with the onset of cold conditions, this paleoenvironmental interval could be matched with MIS 100 to 96 (Fig. 9). These isotope stages mark the first cold stages of the onset of Northern Hemisphere Glaciation (Shackleton et al., 1984; Ruddiman et al., 1986; Raymo et al., 1989; Tiedemann et al., 1994). This interval with its short term fluctuations has been investigated and discussed in more detail by Kuhlmann (2004).

5.3.4.3. Restricted marine (logunit 10 to 12). This interval comprises a significant change in the paleoenvironment towards more restricted marine conditions. The high abundance of and the low diversity of the dinocyst assemblages, together with the enhanced abundance of reworked dinocysts, indicate an important sea-level drop from logunit 10 onward. The erosional surfaces bounding logunits 11 and 12 (Fig. 11) support a low sea-level stand. This sea level drop may be forced by the decrease in temperature since cold climate conditions remain during this interval. The low-diversity foraminiferal assemblages and the impoverished dinocyst assemblages indicate that stressed conditions must have prevailed in connection with unfavourable living conditions for those organisms. We suggest that this facies-related change is not triggered by temperature changes only but by extreme environmental conditions due to the sea level lowering and the restricted-marine conditions, which were periodically already existent in the underlying interval. The benthic assemblages are dominated by either *E. hannai* or *E. excavatum*. *E. excavatum* is a generalistic species that tolerates extreme environmental conditions and has also been found near ablating ice margins on shelf sea areas (Vilks, 1981). This species shows peak occurrences at the base and the top of logunit 10 in our record. At the same levels, the acme occurrences of *O. israelianum* (D7 and D9) represent periods with increased run-off that might be related to such ablation events.

Below and above the gamma-ray peak of logunit 10, *C. laevigata* has two peak occurrences that might be related to temporary open marine conditions since this species has been described from nutrient poor areas in the Atlantic (Rasmussen et al., 2002). However, the presence of *V. fusiformis* at the gamma-ray peak in logunit 10, points to a shallow water depth, as this species lives at present in the inner shelf mud (30 to 40 m water depth) of the southern North Sea (e.g. Moodley, 1990).

Another prominent feature at this level is the peak occurrences of *Artemisia* and *Pediastrum* (P4a and Appendix) which respectively represent open steppe vegetation (Tallis, 1990) and fresh water in small ponds on land. These pollen types were easily transported towards the sea at times of low vegetation cover. Hence, they have been associated with cold climatic conditions and concomitant low vegetation cover. Towards the top of the interval, consistently high proportions of Ericales (P5 to P6) manifest relatively cold climatic conditions during logunits 11 and 12.

During this paleoenvironmental interval, a sudden transition to restricted marine conditions occurred. However, the extremely impoverished faunal assemblages cannot be attributed to the sea level lowering alone. In the present-day situation, the North Sea is shallower than in the Late Pliocene but it is influenced by Atlantic water and a strong anti-clockwise circulation pattern persists (Otto et al., 1990). We suggest that the North Sea circulation ceased during this interval, in such a way that the inflow Atlantic water was reduced to a minimum. The North Sea was strongly influenced by an enormous supply of freshwater from the huge river system in the hinterland, which would then caused a strong haline stratification of the water column. Baumann and Huber (1999) and Henrich et al. (2002) showed that during the time interval from 2.8 to 1.1 Ma warm Atlantic waters were not transported further north than the Iceland–Faroe ridge. The southward movement of the polar front during glacial conditions should have influenced the oceanographic situation and the circulation pattern of the adjacent North Sea as well. With a reduced inflow of Atlantic waters, the North Sea was probably transformed into a semi-estuarium. Such a constellation is very sensitive with respect to temperature, nutrient and salinity changes. Probably, the fluctuations discussed in the previous interval have been first signs toward a sluggish circulation. In summary, we propose a stable freshwater layering for the North Sea with ongoing shallowing and coeval cooling for this interval.

5.3.4.4. Shallow marine, arctic (logunit 13 to logunit 17). The next major shift of climatic conditions is marked by the first occurrence of *H. orbiculare* (F9) at the base of logunit 13. *H. orbiculare* and *E. bartletti* occurring in B17-05 in logunit 16 are typical for river-proximal, arctic environments (Khusid and Korsun, 1996; Polyak et al., 2000). The presence of these species reflects the culmination of the cold conditions and the vicinity of a river system. The ongoing sea level lowering is evident by a peak-abundance of reworked dinocysts at the base of logunit 15. Above that level, sporomorphs dominate over dinocysts indicating a strong fluvial influence. Among the dinocysts, the *Filisphaera* group is most prominent together with *Spiniferites* as the second most abundant species. While the dominance of the (sub-) polar *Filisphaera*/*Habibacysta* group is associated with low SST, the common occurrence of *Spiniferites*, the presence of *A. umbracula* and the overall richness of the assemblages are at the same time indicative for a temporary return of open marine conditions at the base of logunit 15. The same is suggested by the occurrence of *Cassidulina levigata* in two distinct levels, one in logunit 15, and the other in logunit 16. These levels seem to represent punctuations in a long period of relatively restricted conditions, as these are the only *Cassidulina* occurrences since logunit 12. The pollen signal (P6 and P8) with high *Picea* contents in logunit 13 and in logunit 16 reflects short periods of warmer climatic conditions. This signal has to be interpreted more cautiously in terms of climatic conditions because local factors become more prominent in the course of the approaching river system. However, it is puzzling that temporarily warmer conditions prevailed at the same time with high abundance of the (sub) polar *Filipshaera* group. One explanation for the occurrence of these dinocyst species is to treat the assemblage not as an 'in situ' cold signal, but as an allochthonous component, transported into the North Sea during the concurrent open marine conditions. Matthiessen and Brenner (1996) described a *Filisphaera* acme in the Arctic Ocean at the same time, just below the base of the Olduvai chron, which coincides with a melting event at the arctic sea-ice front. From 3D-seismic time slices (Kuhlmann, 2004) a random pattern of straight lineaments and 'scratches' started to develop from logunit 13 onwards. These features were interpreted as scours from icebergs that could have been drifted from the north into the North Sea after a melting period (Kuhlmann, 2004). As a consequence, the dinoflagellates could have been transported either directly by oceanic currents from higher latitudes or incorporated in the icebergs into the North Sea.

During this paleoenvironmental interval, the North Sea became a very shallow basin filled with predominantly low saline waters. Such a setting is very sensitive to temperature changes; a small decrease in temperature is sufficient to cool the watermasses and sea-ice will be formed. Therefore, we propose that a generally stagnant water column persisted under cold climate conditions with the establishment of a (permanent) sea-ice cover, interrupted by warmer intrusions with surface transport directed into the North Sea.

5.3.4.5. Fluvial to deltaic, paralic (logunit 17 and logunit 18). This interval is characterised by strong facies changes because of the continuing shallowing and its position close to the shore. The climatic information from the pollen signal is inconclusive, but since *Picea* is no longer common, the markedly low proportion of thermophilous trees and the high abundance of Ericales (P10) in the southwest of the study area, reflects relatively cold conditions. The foraminiferal low-diversity assemblages are dominated by either *E. excavatum* or *H. orbiculare*, inferring cold climate conditions. Dinocysts are very rare to absent (post D12); instead, fresh-water algae and reworked dinocysts are common, suggesting a fluvial, deltaic to paralic environment within the uppermost-investigated interval of logunit 17 and logunit 18.

6. Conclusions

- The independent biostratigraphic framework based on dinoflagellates, foraminifers and pollen has been tied to the most recent Global Polarity Time Scale (GPTS) of Cande and Kent (1995) and astronomically calibrated ages of Lourens et al. (1996), supported by a continuous geomagnetic record and discrete paleomagnetic measurements. This has resulted in high-resolution age assessment for the sediments above the Middle Miocene Unconformity in the southern North Sea. The succession comprises a thin interval of Middle to Upper Miocene sediments but its main part spans the Pliocene Piacenzian to Gelasian stages, from 3.6 to 1.8 Ma including the paleomagnetic Gauss–Matuyama boundary and (most of) the Olduvai subchron.
- Short paleomagnetic events have been found between the Gauss and Olduvai chronozones. These events can be interpreted either as the Reunion subchron or the X-event. On the basis of the environmental setting, sedimentation rates, and its position close to glacial isotope stage 96, we conclude that the X-event probably has been detected within the investigated succession. The Reunion subchron is recognised near an erosional surface and is therefore less well preserved.
- Best estimate sedimentation rates vary between 30 cm/kyr in the lower part of the succession and up to 84 cm/kyr in the upper part.

– The general paleoenvironmental long-term trend points to a climate cooling and a corresponding overall sea-level lowering. The paleoenvironmental evolution of the southern North Sea during the Late Pliocene has led to the formation of five intervals: 1) open marine, temperate; 2) transitional, cold conditions with warmer intervals; 3) restricted marine; 4) shallow marine, arctic; and 5) fluvial to deltaic, paralic.

Acknowledgements

This research is part of the PhD project of G.K. The funding of this project by Wintershall Noordzee B.V. and its partners Marathon Oil Company, Dana Petroleum and Energie Beheer Nederland (EBN) is gratefully acknowledged. We thank Wintershall Noordzee B.V. and NAM (Nederlandse Aardolie Maatschappij) for providing the offshore samples to this study and for the permission to publish the results. We thank M. Huuse and an anonymous reviewer for their comments which have considerably improved the manuscript. This work has been carried out at the Utrecht University and the Geological Survey of the Netherlands (TNO-NITG) which are thanked for providing archive data and working facilities.

Appendix A. Dinocyst data for wells:

A15-3
B10-3
B13-3
B13-4
B16-1
B17-6

Appendix B. Pollen data for wells:

A18-2
B10-3
B13-3
B16-1
B17-5

Appendix C. Foraminifer data for wells:

B10-3
B13-3
B17-5

Abbreviations: SWC = side wall core; CO = core; CU = cutting

References

Barthés, V., Pozzi, J.P., Vibert-Charbonnel, P., Thival, J., Melieres, M. A., 1999. High-resolution chronostratigraphy from downhole susceptibility logging tuned by palaeoclimatic orbital frequencies. Earth and Planetary Science Letters 165, 97–116.

Baumann, K.-H., Huber, R., 1999. Sea-surface gradients between the North Atlantic and the Norwegian Sea during the last 3.1 m.y.: comparison of sites 982 and 985. In: Raymo, M.E., Jansen, E., Blum, P., Herbert, T.D. (Eds.), Proceedings of the Ocean Drilling Program, Scientific Results, pp. 179–190.

Berggren, W.A., Kent, D.V., Swisher, C.C., Aubry, M-P., 1995. A revised Cenozoic geochronology and chronostratigraphy. Geochronology time scales and global stratigraphic correlation. SEPM Special Publication 54, 129–212.

Bijlsma, S., 1981. Fluvial sedimentation from the Fennoscandian area into the northwest European Basin during the Late Cenozoic. Geologie en Mijnbouw 60, 337–345.

Blakely, R.J., Cox, A., 1972. Evidence for short geomagnetic polarity intervals in the early Cenozoic. Journal of Geophysical Research 77, 7065–7072.

Burger, A.W., 2002. Heavy minerals in the Nieder Ochtenhausen borehole. In: Meyer, K.-J. (Ed.), Forschungsbohrung Nieder Ochtenhausen. Ein Beitrag zur Miozän-Stratigraphie in NW-DeutschlandGeologisches Jahrbuch A, vol. 152, pp. 141–158.

Cameron, T.D.J., Bonny, A.P., Gregory, D.M., Harland, R., 1984. Lower Pleistocene dinoflagellate cyst, foraminiferal and pollen assemblages in four boreholes in the southern North Sea. Geological Magazine 121 (2), 85–97.

Cameron, T.D.J., Stoker, M.W., Long, D., 1987. The history of Quaternary sedimentation in the UK sector of the North Sea Basin. Journal of The Geological Society, London 144, 43–58.

Cameron, T.D.J., Bulat, J., Mesdag, C., 1993. High resolution seismic profile through a Late Cenozoic delta complex in the southern North Sea. Marine and Petroleum Geology 10, 591–599.

Cande, S.C., Kent, D.V., 1992. A new geomagnetic polarity time scale for the Late Cretaceous and Cenozoic. Journal of Geophysical Research 97 (B10), 13917–13951.

Cande, S.C., Kent, D.V., 1995. Revised calibration of the geomagnetic polarity timescale for the Late Cretaceous and Cenozoic. Journal of Geophysical Research 100 (B4), 6093–6095.

Castradori, D., Rio, D., Hilgen, F.J., Lourens, L.J., 1998. The Global Standard Stratotype-section and Point (GSSP) of the Piacenzian stage (Middle Pliocene). Episodes 21 (2), 88–93.

Clausen, O.R., Gregersen, U., Michelsen, O., Sorensen, J.C., 1999. Factors controlling the Cenozoic sequence development in the eastern parts of the North Sea. Journal of The Geological Society, London 156, 809–816.

Dale, B., 1996. Dinoflagellate cyst ecology: modelling and geological applications. In: Jansonius, J.M.G., D.C. (Eds.), Palynology: Principles and Applications. Am. Assoc. Stratgr. Palynol. Foundation, Dallas, Texas, pp. 1249–1275.

Dankers, P.H.M., Zijderveld, J.D.A., 1981. Alternating field demagnetization of rocks, and the problem of gyroremanence. Earth and Planetary Science Letters 53, 89–92.

De Vernal, A., Londeix, L., Mudie, P.J., Harland, R., Morzadec-Kerfourn, M.T., Turon, J.-L., Wrenn, J.H., 1992. Quaternary organic-walled dinoflagellate cysts of the North Atlantic Ocean and adjacent seas: eco-stratigraphy and biostratigraphy. In: Head, M.J.W., J.H. (Eds.), Neogene and Quaternary Dinoflagellate Cysts and Acritarchs. Am. Assoc. Stratgr. Palynol. Foundation, Dallas, Texas, pp. 289–328.

De Vernal, A., Henry, M., Matthiessen, J., Mudie, P.J., Rochon, A., Boessenkool, K.P., Eynaud, F., Grøsfjeld, K., Guiot, J., Hamel, D., Harland, R., Head, M.J., Kunz-Pirrung, M., Evac, E., Loucheur, V., Peyron, O., Pospelova, V., Radi, T., Turon, J.-L., Voronina, E., 2001. Dinoflagellate cyst assemblages as tracers of sea-surface conditions in the northern North Atlantic, Arctic and sub-Arctic seas: the new '$n = 677$' data base and its application for quantitative palaeoceanographic reconstruction. Journal of Quaternary Science 16, 681–698.

De Verteuil, L., Norris, G., 1996. Miocene dinoflagellate stratigraphy and systematics of Maryland and Virginia. Micropaleontology 42 (supplement, 172 pp.).

Doppert, J.W.C., 1980. Lithostratigraphy and biostratigraphy of marine Neogene deposits in the Netherlands. Mededelingen van het Rijks Geological Dienst 32-16, 255–311.

Doppert, J.W.C., Laga, P.G., Meuter, F.J.D., 1979. Correlation of the biostratigraphy of marine Neogene deposits, based on benthonic foraminifera, established in Belgium and the Netherlands. Mededelingen van het Rijks Geological Dienst 31-1, 1–8.

Edwards, L.E., Andrle, V.A.S., 1992. Distribution of selected dinoflagellate cysts in modern marine sediments. In: Head, M.J.W., J.H. (Eds.), Neogene and Quaternary Dinoflagellate Cysts and Acritarchs. Am. Assoc. Stratigr. Palynol. Foundation, Dallas, Texas, pp. 259–288.

Eidvin, T., Riis, F., Rundberg, Y., 1999. Upper Cainozoic stratigraphy in the central North Sea (Ekofisk and Sleipner fields). Geologisk Tidsskrift 79, 97–128.

Etchecopar, A., Thomassin, C., Barthes, V., Pocachard, J., 1994. Geological High-Resolution Magnetic Tool (GHMT) Interpretation Method. Schlumberger Riboud Product Center–IE, LETI/DSYS/CSME.

Evans, D., McGiveron, S., McNeill, A.E., Harrison, Z.H., Østmo, S.R., Wild, J.B.L., 2000. Plio-Pleistocene deposits on the mid-Norwegian margin and their implications for late Cenozoic uplift of the Norwegian mainland. Global and Planetary Change 24, 233–237.

Evans, D., Graham, C., Armour, A., Bathurst, P., 2003. The Millenium Atlas: Petroleum Geology of the Central and Northern North Sea. The Geological Society of London. 389 pp.

Fleet, A.J., Boldey, S.A.R., (Eds.), 1999. Petroleum Geology of Northwest Europe: Proceedings of the 5th Conference. The Geological Society, London. Alden Press, Oxford. 1383 pp.

Funnel, B., 1996. Global sea-level and the (pen-)insularity of late Cenozoic Britain. In: Preece, R.C. (Ed.), Island Britain: a Quaternary Perspective. Geol. Soc. Spec. Pub., 96, pp. 3–13.

Gibbard, P.L., 1988. The history of the great northwest European rivers during the past three million years. Philosophical Transactions of the Royal Society of London. B 318, 559–602.

Gibbard, P.L., West, R.G., Zagwijn, W.H., Balson, P.S., Burger, A.W., Funnel, B.M., Jeffery, D.H., de Jong, J., van Kolfschoten, T., Loster, A.M., Meijer, T., Norton, P.E.P., Treece, R.C., Rose, J., Stuart, A.J., Whiteman, C.A., Zalasiewicz, J.A., 1991. Early and Early Middle Pleistocene correlations in the southern North Sea Basin. Quaternary Science Reviews 10, 23–52.

Glennie, K.W., 1990. Introduction to the Petroleum Geology of the North Sea. Blackwell, Oxford. 402 pp.

Gradstein, F., Backstrøm, S., 1996. Cainozoic biostratigraphy and palaeobathymetry, northern North Sea and Haltenbanken. Norsk Geologisk Tidskrift 76, 3–32.

Gradstein, F.M., Berggren, W.A., 1981. Flysch-type agglutinated foraminifera and the Maastrichtian to Paleogene history of the Labrador and North Seas. Marine Micropaleontology 6, 211–268.

Gradstein, F.M., Kristiansen, I.L., Loemo, L., Kaminski, M., 1992. Cenozoic foraminiferal and dinoflagellate cyst biography of the central North Sea. Micropalaeontology 38, 101–137.

Gradstein, F.M., Kaminski, M.A., Berggren, W.A., Kristiansen, I.L., D'Ioro, M., 1994. Cainozoic biostratigraphy of the North Sea and Labrador Shelf. Micropaleontology 40 (supplement 1994, 152 pp.).

Gramann, F., Kockel, F., 1988. Palaeogeographical, lithological, palaeoecological and palaeoclimatic development of the Northwest European Tertiary Basin. In: Vinken, R. (Ed.), The Northwest European Tertiary BasinGeologisches Jahrbuch, pp. 428–441.

Gregersen, U., 1997. Sequence stratigraphic analysis of Upper Cenozoic deposits in the North Sea based on conventional and 3-D seismic data and well-logs. Aarhus Geoscience Ph.D. Thesis, vol. 5, 167 pp.

Grommé, C.S., Hay, R.L., 1979. Geomagnetic polarity epochs: age and duration of the Olduvai normal polarity event. Earth and Planetary Science Letters 10, 179–185.

Hallam, D.F., Macher, B.A., 1994. A record of reversed polarity carried by the iron sulphide greigite in British early Pleistocene sediments. Earth and Planetary Science Letters 121, 71−80p.

Harland, R., 1979. Dinoflagellate biostratigraphy of Neogene and Quaternary sediments at holes 400/400A in the Bay of Biscay (Deep Sea Drilling Project Leg 8). In: Montadert, L., Roberts, D.G., et al. (Eds.), Initial Reports of the Deep Sea Drilling Project, vol. 48. U.S. Government Printing Office, Washington, D.C., pp. 531–545.

Harland, R., 1992. Dinoflagellate cysts of the Quaternary system. In: Powell, A.J. (Ed.), A Stratigraphic Index of Dinoflagellate Cysts. Chapman and Hall, London, pp. 253–280.

Haq, B.U., Hardenbol, J., Vail, P.R., 1987. Chronology of fluctuating sea levels since the Triassic. Science 235, 1156–1166.

Head, M.J., 1998. Marine environmental change in the Pliocene and early Pleistocene of eastern England: the dinoflagellate evidence reviewed. Mededelingen Nederland Instituut voor Teogepaste Geowetenschappen TNO 60, 199–225.

Heirtzler, J.R., Dickson, G.O., Herron, E.M., Pitman, W.C., LePichon, X., 1968. Marine magnetic anomalies, geomagnetic field reversals and motions of the ocean floor and continents. Journal of Geophysical Research 73, 2119–2136.

Henrich, R., Baumann, K.H., Huber, R., Meggers, H., 2002. Carbonate preservation records of the past 3 Myr in the Norwegian–Greenland Sea and the northern North Atlantic: implications for the history of NADW production. Marine Geology 184 (1–2), 17–39.

Henriksen, S., Vorren, T.O., 1996. Late Cenozoic sedimentation and uplift history on the mid-Norwegian continental shelf. Global and Planetary Change 12, 171–199.

Huuse, M., 2002. Late Cenozoic palaeogeography of the eastern North Sea Basin: climate vs. tectonic forcing of basin margin uplift and deltaic progradation. Bulletin of the Geological Society of Denmark 49, 145–170.

Huuse, M., Clausen, O.R., 2001. Morphology and origin of major Cenozoic sequence boundaries in the eastern North Sea Basin: top Eocene, near-top Oligocene and the mid-Miocene unconformity. Basin Research 13, 17–41.

Huuse, M., Lykke-Andersen, H., Michelsen, O., 2001. Cenozoic evolution of the eastern North Sea Basin — new evidence from high-resolution and conventional seismic data. Marine Geology 177, 243–269.

Jordt, H., Faleide, J.I., Bjørlykke, K., Ibrahim, M.T., 1995. Cenozoic sequence stratigraphy of the central and northern North Sea Basin:

tectonic development, sediment distribution and provenance areas. Marine and Petroleum Geology 12 (8), 845–879.

Kasse, C., 1996. Paleomagnetic dating and effects of Weichselian periglacial processes on the magnetization of early Pleistocene deposits (southern Netherlands, northern Belgium). Geolgie en Mijnbouw 75 (19–31 pp.).

Khusid, T.K., Korsun, S.A., 1996. Modern benthic foraminiferal assemblages in the Kara Sea. Berichte zur Polarforschung 212, 308–314.

King, C., 1983. Cainozoic micropalaeontological biostratigraphy of the North Sea. Report Institute Geological Sciences 82, 1–40 (6 pl.).

King, C., 1989. Cenozoic of the North Sea. In: Jenkins, D.G., Murray, J.W. (Eds.), Stratigraphical Atlas of Fossil Foraminifera. Ellis Horwood, Chichester, pp. 418–489.

Konradi, P.B., 1996. Foraminiferal biostratigraphy of the post-mid Miocene in the Danish Central Trough, North Sea. In: De Batist, M.P.J. (Ed.), Geology of Siliclastic Shelf Seas. Geol. Soc. Spec. Publ.

Kooi, H., Hettema, M., Cloetingh, S., 1991. Lithosperic dynamics and the rapid Pliocene–Quaternary subsidence phase in the southern North Sea Basin. Tectonophysics 192, 245–259.

Kristofferson, F.N., Bang, I., 1982. Cenozoic excl. Danian limestone. In: Michelsen, O. (Ed.), Geology off the Danish Central Graben. Danmarks Geol. Unders. Series, B, vol. 8, pp. 61–70.

Kuhlmann, G., 2004. High resolution stratigraphy and paleoenvironmental changes in the southern North Sea during the Neogene — an integrated study of Late Cenozoic marine deposits from the northern part of the Dutch offshore area. http://igitur-archive.library.uu.nl/dissertations/2005-0511-200057/UUindex.html. Ph.D. thesis, Utrecht University, Geologica Ultraiectina, Mededelingen van de Faculteit Aardwetenschappen, No. 245, 205 pp.

Laberg, J.S., Stoker, M.S., Dahlgren, K.I.T., de Haas, H., Haflidason, H., Hjelstuen, B.O., Nielsen, T., Shannon, P.M., Vorren, T.O., van Weering, T.C.E., Ceramicola, S., 2005. Cenozoic alongslope processes and sedimentation on the NW European Atlantic margin. Marine and Petroleum Geology 1–20. doi:10.1016/j.marpetgeo.2005.01.008 xx.

Langereis, C.G., Linssen, J.H., Mullender, T.A.T., Zijderveld, J.D.A., 1989. Demagnetization. In: James, D.E. (Ed.), The Encyclopedia of Solid Earth Geophysics. Van Nostrand Reinhold Company, New York, pp. 201–211.

Laursen, G.V., 1995. Foraminiferal analyses of Tertiary deposits in the North Sea area: stratigraphy, palaeoecology and taxonomy. Ph.D. thesis, University of Aarhus, 267 pp.

Londeix, L., Benzakour, M., de Vernal, A., Turon, J.-L., Suc, J-P., 1999. Late Neogene dinoflagellate cyst assemblages from the Strait of Sicily, central Mediterranean Sea: paleo-ecological and biostratigraphical implications. In: Wrenn, J.H., Suc, J.-P., Leroy, S.A.G. (Eds.), The Pliocene: Time of Change. American Association of Stratigraphic Palynologists Foundation, pp. 65–91.

Lourens, L.J., Hilgen, F.J., Zachariasse, W.J., van Hoof, A.A.M., Antonarakou, A., Vergnaud-Grazzini, C., 1996. Evaluation of the Pliocene to early Pleistocene astronomical time scale. Paleoceanography 11, 391–413.

Maslin, M.A., Li, X-S., Loutre, M-F., Berger, A., 1998. The contribution of orbital forcing to the progressive intensification of northern hemisphere glaciation. Quaternary Science Review 17 (4–5,), 411–426.

Matthiessen, J., Brenner, W., 1996. Dinoflagellate cyst ecostratigraphy of Pliocene–Pleistocene sediments from the Yermak Plateau (Arctic Ocean, Hole 911A). In: Thiede, H., Myhre, A.M., Firth, J.V., Johnson, G.L., Ruddiman, W.F. (Eds.), Proc. ODP, Sci. Results, vol. 151. Ocean Drilling Program, College Station, TX, pp. 243–253.

Michelsen, O., Danielsen, M., Heilmann-Clausen, C., Jordt, H., Laursen, G.V., Thomsen, E., 1995. Occurrence of major sequence stratigraphic boundaries in relation to basin development in Cenozoic deposits of the southeastern North Sea. In: Steel, R.J., Felt, W.L., Johannessen, E. P., Mathieu, C. (Eds.), Sequence Stratigraphy: Advances and Applications for Exploration and Producing in North West Europe. Norw. Petr. Soc. Elsevier, Amsterdam, pp. 415–427.

Michelsen, O., Thomsen, E., Danielsen, M., Heilmann-Clausen, C., Jordt, H., Laursen, G-V., 1998. Cenozoic sequence stratigraphy in eastern North Sea. In: Graciansky, C.D., Jaquin, T., Vail, P.R., Farley, M.B. (Eds.), Mesozoic and Cenozoic Sequence Stratigraphy of European Basins. Soc. Econ. Pal. Min. (SEPM), Spec. Pub., pp. 91–118.

Moodley, L., 1990. Southern North Sea seafloor and subsurface distribution of living benthic Foraminifera. Netherlands Journal of Sea Research 27 (1), 57–71.

Mudie, P.J., 1989. Palynology and dinocyst biostratigraphy of the late Miocene to Pleistocene, Norwegian Sea ODP Leg 104, Sites 642 to 644. In: Eldholm, O., Thiede, J., Tayler, E., et al. (Eds.), Proceedings of the Ocean Drilling Program, College Station, Texas.

Murray, J.W., 1991. Ecology and Palaeoecology of Benthic Foraminifera. Longman Group UK Limited. 380 pp.

Otto, L., Zimmerman, J.T.F., Furnes, G.K, Mork, M., Saetre, R., Becker, G., 1990. Review of the physical oceanography of the North Sea. Netherlands Journal of Sea Research 26 (2–4), 161–238.

Overeem, I., Weltje, G.J., Bishop-Kay, C., Kroonenberg, S.B., 2001. The Late Cenozoic Eridanos delta system in the southern North Sea Basin: a climate signal in sediment supply? Basin Research 13, 293–312.

Parker, J.R., 1993. Petroleum Geology of Northwest Europe: Proceedings of the 4th Conference. The Geological Society, London. Alden Press, Oxford. 1527 pp.

Peizhnen, Z., Molnar, P., Downs, W.R., 2001. Increased sedimentation rates and grain sizes 2–4 Myr ago due to the influence of climate change on erosion rates. Nature 410, 891–897.

Polyak, L., Levitan, M., Gataullin, V., Kushid, T., Mikhailov, V., Mukhina, V., 2000. The impact of glaciation, river-discharge and sea-level change on Quaternary environments in the southwestern Kara Sea. Journal of International Earth Science 89 (3), 550–562.

Poulsen, N.E., Manum, S.B., Williams, G.L., Ellegaard, M., 1996. Tertiary dinoflagellate biostratigraphy of Sites 907, 908 and 909 in Norwegian–Greenland Sea. In: In Thiede, J., Myhre, A.M., Firth, J.V., Johnson, G.L., Ruddiman, W.F. (Eds.), Proc. ODP, Sci. Res., College Station, TX (Ocean Drilling Program), pp. 255–287.

Pozzi, J.-P., Barthes, V., Thibal, J., Pocachard, J., Lim, M., Thomas, T., Pages, G., 1993. Downhole magnetostratigraphy in sediments: comparison with the paleomagnetism of a core. Journal of Geophysical Research 98 (B5), 7939–7957.

Rasmussen, T.L., Backstrom, D., Heinemeier, J., Klitgaard-Kristensen, D., Knutz, P.C., Kuijpers, A., Lassen, S., Thomsen, E., Troelstra, S.R., 2002. The Faroe–Shetland Gateway: Late Quaternary water mass exchange between the Nordic seas and the northeastern Atlantic. Marine Geology 188, 165–192.

Raymo, M.E., Ruddiman, W.F., 1992. Tectonic forcing of late Cenozoic climate. Nature 359, 117–122.

Raymo, M.E., Ruddiman, W.F., Backman, J., Clement, B.M., Martinson, D.G., 1989. Late Pliocene variation in northern hemisphere ice sheets and North Atlantic deep water circulation. Paleoceanography 4, 413–446.

Rea, D.K., Blakely, R.J., 1975. Short-wavelength anomalies in a region of rapid seafloor spreading. Nature 255, 126–128.

Rochon, A., de Vernal, A., Turon, J.-L., Matthiessen, J., Head, M.J., 1999. Distribution of dinoflagellate cyst assemblages in surface sediments from the North Atlantic Ocean and adjacent basins and quantitative reconstruction of sea-surface parameters. Special Contribution Series, vol. 35. American Association of Stratigraphic Palynologists, Dallas, TX.

Ruddiman, W.F., Raymo, M., McIntyre, A., 1986. Matuyama 41,000-year cycles: North Atlantic Ocean and northern hemisphere ice sheets. Earth and Planetary Science Letters 80, 117–129.

Shackleton, N.J., Backman, J., Zimmerman, J., Kent, D.V., Hall, M.A., Roberts, D.G., Schnitker, D., Baldaud, J.G., Desprairies, A., Homrighausen, R., Keene, J.B., Kaltenbakc, A..J., Krumsiek, K.A.O., Morton, A.C., Murray, J.W., Westberg-Smith, J., 1984. Oxygen isotope calibration of the onset of ice-rafting and history of glaciation in the North Atlantic region. Nature 307, 620–623.

Smelror, M., 1999. Plio-Pleistocene and redeposited dinoflagellate cysts from the western Svalbard Margin (Site 986): biostratigraphy, paleoenvironment and sediment provenance. In: Raymo, M.E., Jansen, E., Blum, P., Herbert, T.D. (Eds.), Proc. ODP, Sci. Res., College Station, TX (Ocean Drilling Program), pp. 83–97.

Spiegler, D., 1999. Bolboforma biostratigraphy from the Hatton–Rockall Basin (North Atlantic). In: Raymo, M.E., Jansen, E., Blum, P., Herbert, T.D. (Eds.), Proceedings ODP, Scientific Results, vol. 162. Ocean Drilling Program, College Station, TX, pp. 35–49.

Spiegler, D., Jansen, E., 1989. Planktonic foraminifer biostratigraphy of Norwegian Sea sediments: ODP leg 104. In: Eldholm, O., Thiede, J., Tayler, E., et al. (Eds.), Proceedings of the Ocean Drilling Program, Scientific Results, pp. 681–696.

Spiegler, D., von Daniels, C.H., 1991. A stratigraphic and taxonomic atlas of Bolboforma (Protophytes, Incertae Sedis, Tertiary). Journal of Foraminiferal Research 21, 126–158.

Stoker, M.S., Nielsen, T., van Weering, T.C.E., Kuijpers, A., 2002. Towards an understanding of the Neogene tectonostratigraphic framework of the NE Atlantic Margin between Ireland and the Faroe Islands. Marine Geology 188 (1–2), 233–248.

Streif, H. (Ed.), 1996. Deutsche Beitrage zur Quartärforschung in der südlichen Nordsee. Geologisches Jahrbuch, Heft, 146. Reihe A. E. Schweizerbart'sche Verlagsbuchhandlung, Hannover. 244 pp.

Sørensen, J.C., Michelsen, O., 1995. Upper Cenozoic sequences in the south-eastern North Sea Basin. Bulletin of the Geological Society of Denmark 42, 74–95.

Sørensen, J.C., Gregersen, U., Breiner, M., Michelsen, O., 1997. High-frequency sequence stratigraphy of Upper Cenozoic deposits in the central and southeastern North Sea areas. Marine and Petroleum Geology 14 (2), 99–123.

Tallis, 1990. Climate Change and Plant Communities. Academic press, London.

Thiede, J., Winkler, A., Wolf-Welling, T., Eldholm, O., Myhre, A.M., Baumann, K.-H., Henrich, R., Stein, R., 1998. Late Cenozoic history of the polar North Atlantic: results from ocean drilling. Quaternary Science Reviews 17, 185–208.

Tiedemann, R., Sarnthein, M., Shackleton, N.J., 1994. Astronomic timescale for the Pliocene Atlantic delta-O-18 and dust flux. Paleoceanography 9 (4), 619–638.

Traverse, A., 1988. Production, dispersal, and sedimentation of spores/pollen. In: Traverse, A. (Ed.), Paleopalynology. Unwin Hyman, Boston, pp. 375–430.

Vail, P.R., 1987. Seismic stratigraphy interpretation using sequence stratigraphy, part 1: seismic stratigraphy interpretation procedure. In: Bally, A.W.E. (Ed.), Atlas of Seismic Stratigraphy. Am. Ass. Petr. Geol., pp. 1–13.

Van Wagoner, J.C., Mitchum, R.M., Campion, K.M., Rahmanian, V.D., 1990. Siliciclastic sequence stratigraphy in well logs, cores and outcrops: concepts for high-resolution correlation of time and facies. AAPG Methods in Exploration Series 7 (55 pp.).

Versteegh, G.J.M., 1995. Paleoenvironmental changes in the Mediterranean and North Atlantic in relation to the onset of northern hemisphere glaciations — a palynological approach. Published thesis, University of Utrecht, Ponsen en Looijen, Wageningen. 134 pp.

Vilks, G., 1981. Late Glacial–postglacial foraminiferal boundary in sediments of eastern Canada, Denmark and Norway. Geoscience Canada 8 (2), 48–55.

Vinken, 1988. The North West European Tertiary Basins. Results of the international geological correlation programme, project no. 124. Geologisches Jahrbuch 100 (508 pp.).

Von Daniels, C.H., 1986. Uvigerina in the NW European Neogene. In: van der Zwaan, G.J., Jorissen, F.J., Verhallen, P.J.J.M., von Daniels, C.H. (Eds.), Atlantic–European Oligocene to Recent Uvigerina. Utrecht Micropaleontological Bulletin, vol. 35, pp. 67–119.

Weaver, P.P.E., Clement, B.M., 1986. Synchronicity of Pliocene planktonic foraminiferid datums in the North Atlantic. Marine Micropalaeontology 10, 295–307.

Wolf, T.C.W., Thiede, J., 1991. History of terrigenous sedimentation during the past 10 m.y. in the North Atlantic (ODP legs 104 and 105 and DSDP leg 81). Marine Geology 101, 83–102.

Wolf-Welling, T.C.W., Cremer, M., O'Connell, S., Winkler, A., Thiede, J., 1996. Cenozoic Arctic gateway paleoclimate variability: indications from changes in coarse-fraction composition. In: Thiede, J., Myhre, A., Firth, J., Johnson, G.L., Ruddiman, W.F. (Eds.), Proceedings of the Ocean Drilling Program, Scientific Results, vol. 151. Ocean Drilling Program, College Station, Tex, pp. 515–567.

Zachariasse, W.J., Gudjonsson, L., Hilgen, F.J., Langereis, C.G., Lourens, L.J., Verhallen, P.J.J.M., Zijderveld, J.D.A., 1990. Late Gauss to Early Matuyama invasions of *Neogloboquadrina atlantica* in the Mediterranean and associated records of climatic change. Paleoceanography 5, 239–252.

Zagwijn, W.H., 1963. Pollen-analytic investigations in the Tiglian of the Netherlands. Mededelingen Geologische Stichting 16, 49–71 N.S.

Zagwijn, W.H., 1989. The Netherlands during the Tertiary and the Quarternary: a case history of coastal lowland evolution. Geologie en Mijnbouw 68, 107–120.

Ziegler, 1990. Geological Atlas of Western and Central Europe. 3rd edition. Shell International Petroleum Maatschappij B.V. 239 pp.

Zijderveld, J.D.A., 1967. Demagnetization of rocks: analysis of results. In: Collinson, D.W., Creer, K.M., Runcorn, S.K. (Eds.), Methods in Paleomagnetism. Elsevier, pp. 254–286.